NASA TECHNICAL NOTE

NASA TN D-2438

FREE-FLIGHT TEST RESULTS ON THE PERFORMANCE OF CORK AS A THERMAL PROTECTION MATERIAL

by Randolph A. Graves, Jr., and Thomas E. Walton, Jr.

Langley Research Center
Langley Station, Hampton, Va.

NATIONAL AERONAUTICS AND SPACE ADMINISTRATION • WASHINGTON, D. C. • SEPTEMBER 1964

FREE-FLIGHT TEST RESULTS ON THE PERFORMANCE OF CORK AS A THERMAL PROTECTION MATERIAL

By Randolph A. Graves, Jr., and Thomas E. Walton, Jr.

Langley Research Center
Langley Station, Hampton, Va.

NATIONAL AERONAUTICS AND SPACE ADMINISTRATION

For sale by the Office of Technical Services, Department of Commerce,
Washington, D.C. 20230 -- Price $1.00

FREE-FLIGHT TEST RESULTS ON THE PERFORMANCE OF CORK AS A THERMAL PROTECTION MATERIAL

By Randolph A. Graves, Jr., and Thomas E. Walton, Jr.
Langley Research Center

SUMMARY

A series of flight tests was initiated by the Langley Research Center for the purpose of testing ablative cork as a lightweight thermal protection material. These flight tests were conducted aboard NASA flight vehicles in the low-heating-rate environment of the afterbody regions. The test conditions covered a range of altitudes to 482,000 feet and velocities to 17,900 feet per second. The test results show that cork can provide adequate thermal protection for a long-time, low-heating-rate environment.

INTRODUCTION

During ascent and reentry of a high-speed flight vehicle, thermal protection against aerodynamic heating is of prime importance for its survival. Present-day materials used for thermal protection (Teflon, glass phenolic, etc.) tend to be heavy, so that adequate thermal protection is gained at the expense of useful payload weight; therefore, a lightweight thermal protection material appears to be desirable.

An investigation in an arc-heated air jet has been made by the Aeronautical Systems Division of the U.S. Air Force with the objective of determining the ablative characteristics of cork. A similar investigation was the subject of reference 1. Since the simulation of actual flight conditions in ground facilities is seldom achieved, a flight-test program was initiated at the Langley Research Center to obtain performance data on cork as a thermal protection material in an actual flight environment. The cork flight tests were conducted as secondary experiments on five NASA flight vehicles, one of which contained a payload recovery system. The test vehicles either carried instrumented cork patches, or cork was applied to entire sections where thermal protection was required. The experiments were confined to the afterbody regions of the test vehicles where the convective heating rates were relatively low. Data were obtained from four of the flight tests by onboard telemetry systems and from the recovery model by physical examination after recovery. The tests were conducted at altitudes to 482,000 feet, and velocities to 17,900 feet per second were obtained. Maximum values of the velocity, dynamic pressure, and total enthalpy for each test are given in table I. The purpose of this report is to present the results obtained from the five flight tests.

VEHICLE SYSTEMS AND TEST RESULTS

Scout

The NASA Scout vehicle consists of four stages of solid-propellant rocket motors with an Algol and a Castor motor as the first and second stages, respectively. The third and fourth stages are an Antares and an Altair motor, respectively. A photograph of the Scout launch vehicle is shown as figure 1.

Scout 115.- Carried aboard NASA Scout 115 were two instrumented patches of phenolic cork. Phenolic cork is a composite of 80 percent ground cork and 20 percent phenolic resin which has a specific weight of 30 pounds per cubic foot. A 10- by 10- by 0.033-inch cork patch was located on the lower transition D section door with a thermistor placed on the inside surface of the 0.050-inch-thick stainless-steel door, as shown in figure 2. The other cork patch, which is shown in figure 3, had dimensions of 6 inches by 8 inches by 0.033 inch and was located on the upper transition C section skin with a thermistor placed at the interface of the skin and cork. (Transition C is the inner-stage hardware between the second and third stages. Transition D is the inner-stage hardware between the third and fourth stages.) The two cork patches were bonded and faired to transition D section door and transition C section skin by using epoxy adhesives.

The data period for the cork patches extends to about 140 seconds and covers the early ascent portion of the flight trajectory and the period of maximum heating. The aerodynamic heating on the Scout vehicle is a maximum at first-stage burnout (about 60 seconds after launch). The variation of flight velocity and altitude extending through the data period is shown in figure 4. Shown in figure 5 are the measured atmospheric conditions. Since the vehicle exceeded the altitude limit of these measured conditions, values from the 1962 U.S. Standard Atmosphere (ref. 2) are also plotted for the test trajectory.

Figure 6 affords a comparison of temperature histories for transition C and D sections, with and without the cork patches. Figure 6(a) shows the calculated inside-surface temperature without the cork patch and the measured inside-surface temperature with the cork patch on the transition D section. The values of the inside-surface temperature were calculated according to the theory of Van Driest for a turbulent boundary layer (ref. 3) by using local conditions computed by the conical-theory methods of reference 4. Figure 6(b) shows the calculated outside-surface temperature without the cork patch and the measured outside-surface temperature under the cork patch on transition C section. The calculated outside-surface temperatures were also obtained according to the Van Driest turbulent-heat-transfer theory of reference 3 by using free-stream conditions.

Scout 116.- Scout 116 carried a single instrumented cork patch on the upper transition C section skin. This patch was 8 inches by 8 inches by 0.030 inch in dimensions and had a thermistor located at the interface of the cork and skin. Two other thermistors were placed on the inside surface of transition C section. One of these was located under the cork patch and the other was adjacent to the cork patch. (See fig. 7 for details.)

The flight trajectory for Scout 116 was very similar to that for Scout 115. The variation of flight velocity and altitude for Scout 116 is shown in figure 8 for 180 seconds of flight. The measured and standard atmospheric conditions for this flight are presented in figure 9. Figure 10 shows the temperature time histories of the three thermistors for 180 seconds of flight.

RAM B

The RAM B is a solid-propellant three-stage vehicle system. The first- and second-stage motors are a Castor and an Antares, respectively, and the third-stage motor is an Alcor. A photograph of the RAM B vehicle is shown as figure 11.

RAM B1.- The RAM B1 vehicle carried two identical instrumented patches of cork which were located 180° apart on the third-stage flare section. A sketch of the third stage with pertinent dimensions and cork-patch locations is shown in figure 12. Both patches had dimensions of approximately 5 inches by 10 inches by 0.13 inch. The instrumentation for the first patch on the third-stage flare consisted of a slug-type calorimeter (fig. 13) which was used to obtain the magnitude of the local heat flux. The second cork-patch instrumentation consisted of a chromel-alumel thermocouple which was attached to a 1-inch-diameter by 0.030-inch-thick 2S aluminum disk in an attempt to gain a more accurate temperature measurement. This thermocouple assembly was located inside the cork patch 0.07 inch from the outer surface. (See fig. 14.)

The planned flight trajectory of the RAM B1 was not achieved, since a system failure occurred after second-stage ignition (about 45 seconds after launch). However, the data period extends to 70 seconds. The velocity and altitude histories obtained for this flight are shown in figure 15. The measured atmospheric conditions for the flight trajectory are shown in figure 16. Maximum aerodynamic heating during ascent occurred near the time of first-stage burnout; therefore, the system failure did not affect the period of maximum heating. The temperature history of the calorimeter is shown in figure 17. The heating rate as calculated from the calorimeter temperature history is shown in figure 18(a). The response of the thermocouple assembly to this heating rate is shown in figure 18(b). The heating rate was calculated according to the following relation:

$$\dot{Q} = C\frac{dT}{dt} + K\Delta T$$

where

$\dot{Q}$ heating rate, Btu/sq ft-sec

C sensitivity constant, 0.311 (manufacturer's calibration)

$\frac{dT}{dt}$ slope of calorimeter temperature-time curve

K thermal-loss coefficient, 0.0045 (manufacturer's calibration)

ΔT temperature rise of calorimeter

RAM B2.- Cork was applied to the entire third-stage flare of the RAM B2 vehicle for necessary thermal protection. The cork instrumentation consisted of two chromel-alumel thermocouples and an asymptotic calorimeter. The calorimeter and one thermocouple were located 7 inches from the trailing edge of the flare; the other thermocouple was located 2 inches from the trailing edge. (See figs. 19 and 20 for the calorimeter and thermocouple installations.)

The RAM B2 flew successfully throughout the performance range of the vehicle system and reached the highest velocity recorded for the cork tests. The velocity and altitude histories are shown in figure 21. The measured and standard atmospheric conditions for the flight are shown in figure 22. The heating-rate history, as shown in figure 23(a), covers the entire ascent phase and partial reentry phase of the vehicle trajectory. The temperature histories for the two thermocouples responding to essentially the measured heat inputs are shown in figure 23(b).

Payload Recovery Vehicle

The payload recovery vehicle consists of a four-stage, solid-propellant rocket system. This system consists of the following motors: first stage, Honest John; second stage, Nike; third stage, Skat; and fourth stage, Recruit. Figure 24 is a photograph of a four-stage payload recovery vehicle. The recoverable payload consisted of a 10° cone with a hemispherical nose tip and a cylindrical afterbody section. A sketch of the payload is presented as figure 25.

Upon recovery of an earlier identical payload that was subjected to the same test environment, it was observed that the epoxy ablation material had severely ablated at the cone-cylinder juncture (ref. 5). To provide further thermal protection, phenolic cork was applied at this critical location. This cork was 0.25 inch thick by 8 inches wide, was bonded by an epoxy adhesive to the entire periphery on the forward portion of the cylindrical afterbody section, and carried no instrumentation. Figure 26 is a preflight photograph of the recoverable payload showing the cork location and appearance.

The desired trajectory apogee and test conditions for the recovery vehicle were obtained by igniting the first two stages during vehicle ascent, and the last two stages were ignited during descent to obtain the desired reentry test environment. The altitude and velocity histories obtained from radar and accelerometer measurements are shown in figure 27. The measured atmospheric conditions for this flight are shown in figure 28. Prior to termination of the flight test, a parachute was deployed and the velocity of the recoverable payload was decreased to approximately 60 feet per second before water impact.

A photograph of the recovered payload is shown as figure 29. It can be seen that the hemispherical nose eroded to a conical shape during the reentry.

The epoxy ablation material on the conical afterbody came off during the terminal portion of the flight (about 98 seconds after launch), leaving the cork with a blunted leading edge exposed to the air stream; however, the cork prevented further destruction of the epoxy ablation material on the cylindrical afterbody.

Postflight measurements of the cork cross sections showed a char-layer thickness of approximately 0.010 inch. The amount of cork lost during the flight is shown in figure 30.

CONCLUDING REMARKS

A series of five flight experiments was conducted aboard the NASA Scout, RAM, and four-stage research vehicles for the purpose of testing lightweight phenolic cork as a thermal protection material. These tests were carried out in the low-heating-rate environment of the afterbody regions on the vehicles. The test conditions covered a range of altitudes to 482,000 feet and velocities to 17,900 feet per second. Temperature and heating-rate histories were obtained from continuously measured in-flight quantities, whereas ablative performance for the cork on the recovery model was determined from postflight measurements.

The cork patches applied to the Scout vehicles provided a substantial reduction in the aerodynamic heating experienced by the vehicles during the ascent phase of the trajectory.

The results obtained from the RAM B flight tests show that cork can provide adequate thermal protection for a long-time, low-heating-rate environment.

The cork on the recovery model experienced char and erosion; however, it prevented the destruction of the epoxy ablation material on the cylindrical afterbody.

Langley Research Center,
National Aeronautics and Space Administration,
Langley Station, Hampton, Va., May 4, 1964.

REFERENCES

1. Vojvodich, Nick S., and Winkler, Ernest L.: The Influence of Heating Rate and Test Stream Oxygen Content on the Insulation Efficiency of Charring Materials. NASA TN D-1889, 1963.

2. Anon.: U.S. Standard Atmosphere, 1962. NASA, U.S.Air Force, and U.S. Weather Bureau, Dec. 1962.

3. Van Driest, E. R.: The Problem of Aerodynamic Heating. Aero. Eng. Rev., vol. 15, no. 10, Oct. 1956, pp. 26-41.

4. Ames Research Staff: Equations, Tables, and Charts for Compressible Flow. NACA Rep. 1135, 1953. (Supersedes NACA TN 1428.)

5. Lawrence, George F., Whitlock, Charles H., and Walton, Thomas E., Jr.: Aerothermal Measurements of Damaged Reentry Bodies Obtained in Free Flight at Mach Numbers From 11.0 to 2.0. NASA TM X-966, 1964.

TABLE I.- MAXIMUM TEST CONDITIONS

[Reference time is from launch]

Flight tests	Velocity, ft/sec	Dynamic pressure, lb/sq ft	Total enthalpy, Btu/lb
Scout 115	9,900	2,304 (Time = 39 sec)	2,080
Scout 116	10,900	2,026 (Time = 42 sec)	2,770
RAM B1	4,100	6,350 (Time = 30 sec)	430
RAM B2	17,900	6,250 (Time = 29 sec)	6,520
Recoverable model	10,650	12,400 (Time = 91 sec)	2,360

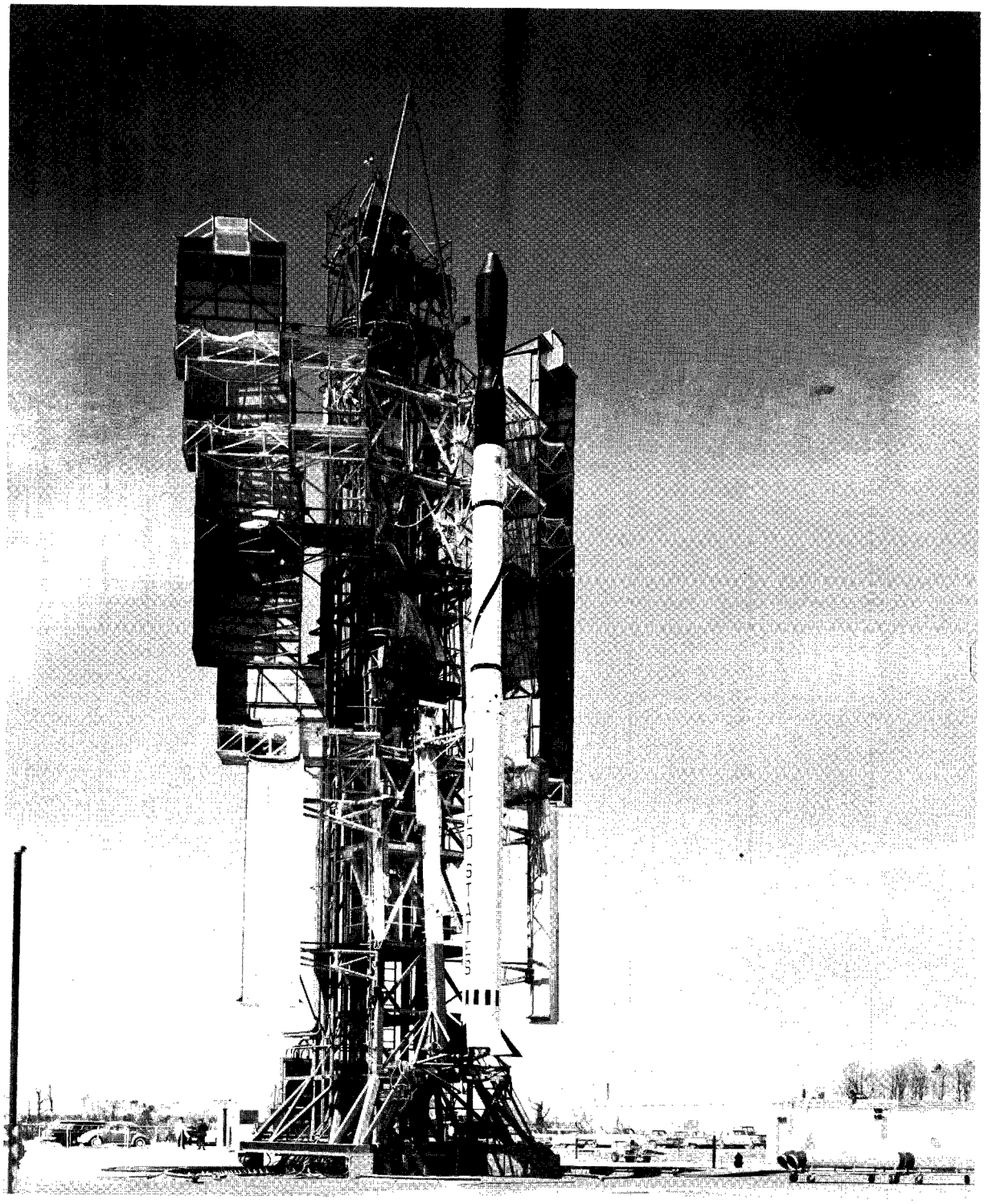

Figure 1.- Scout vehicle. L-63-3475

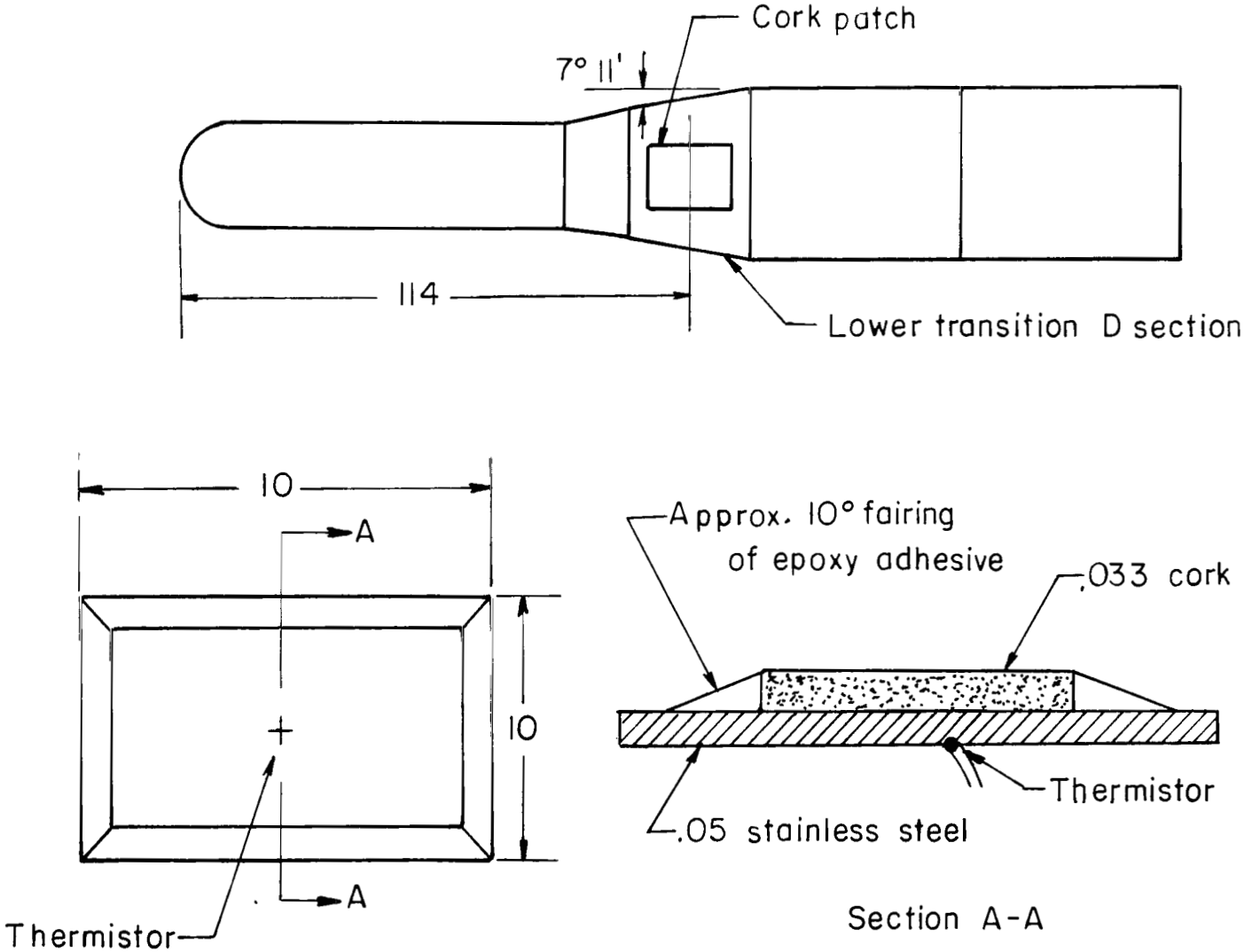

Figure 2.- Cork-patch installation on lower transition D section of Scout 115.
(All dimensions are in inches unless otherwise indicated.)

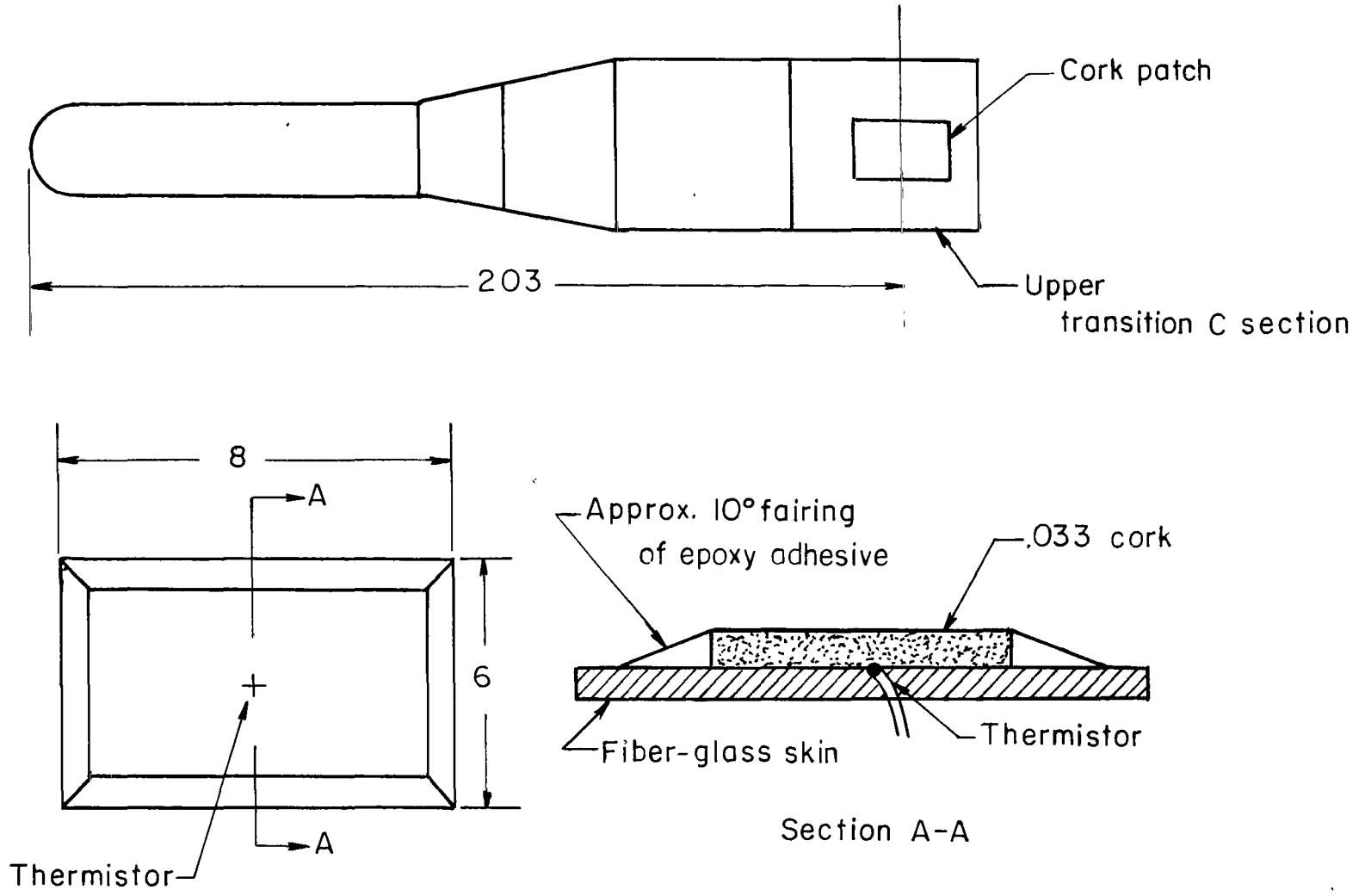

Figure 3.- Cork-patch installation on upper transition C section of Scout 115.
(All dimensions are in inches unless otherwise indicated.)

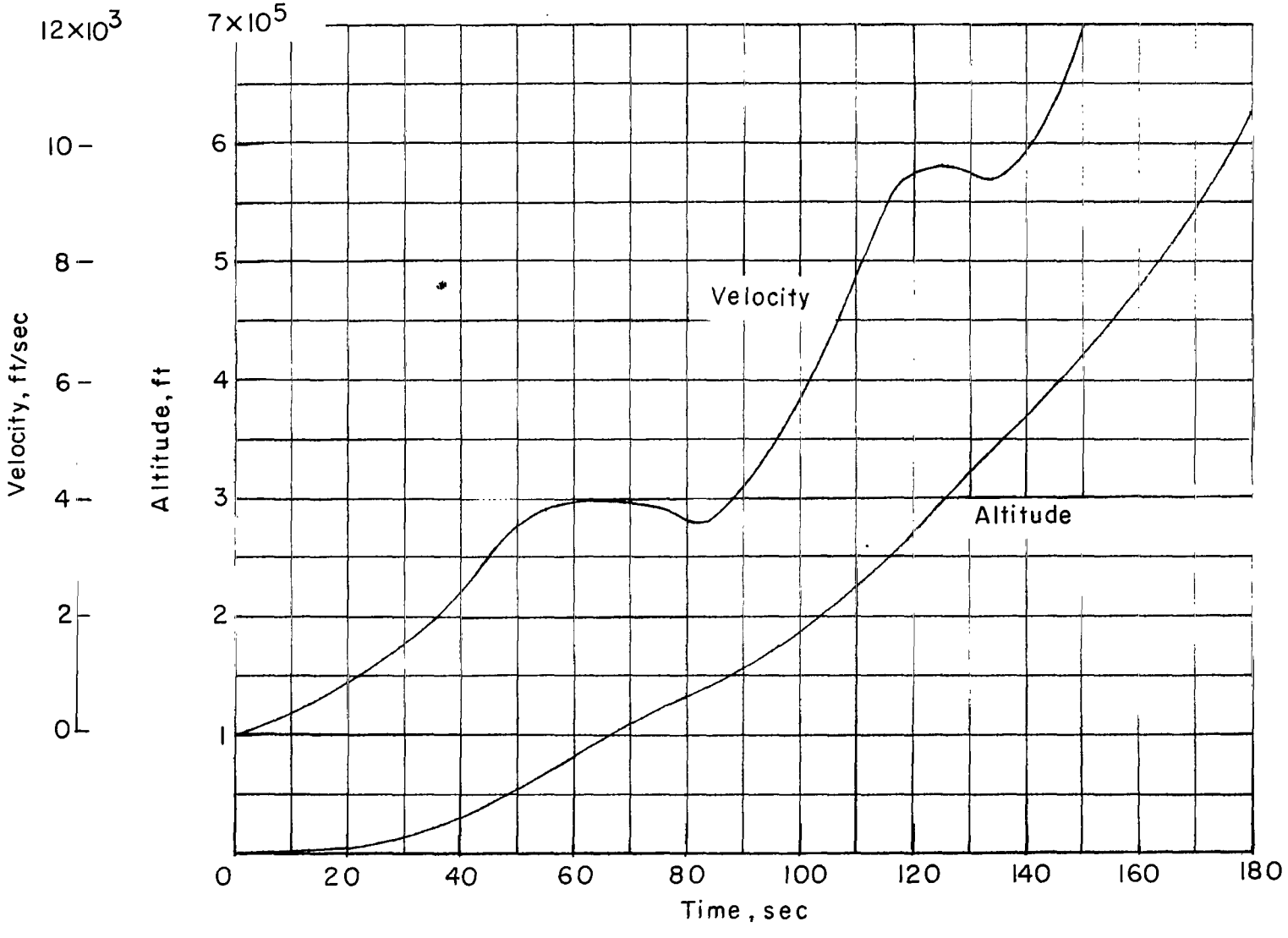

Figure 4.- Velocity and altitude histories for Scout 115 flight test.

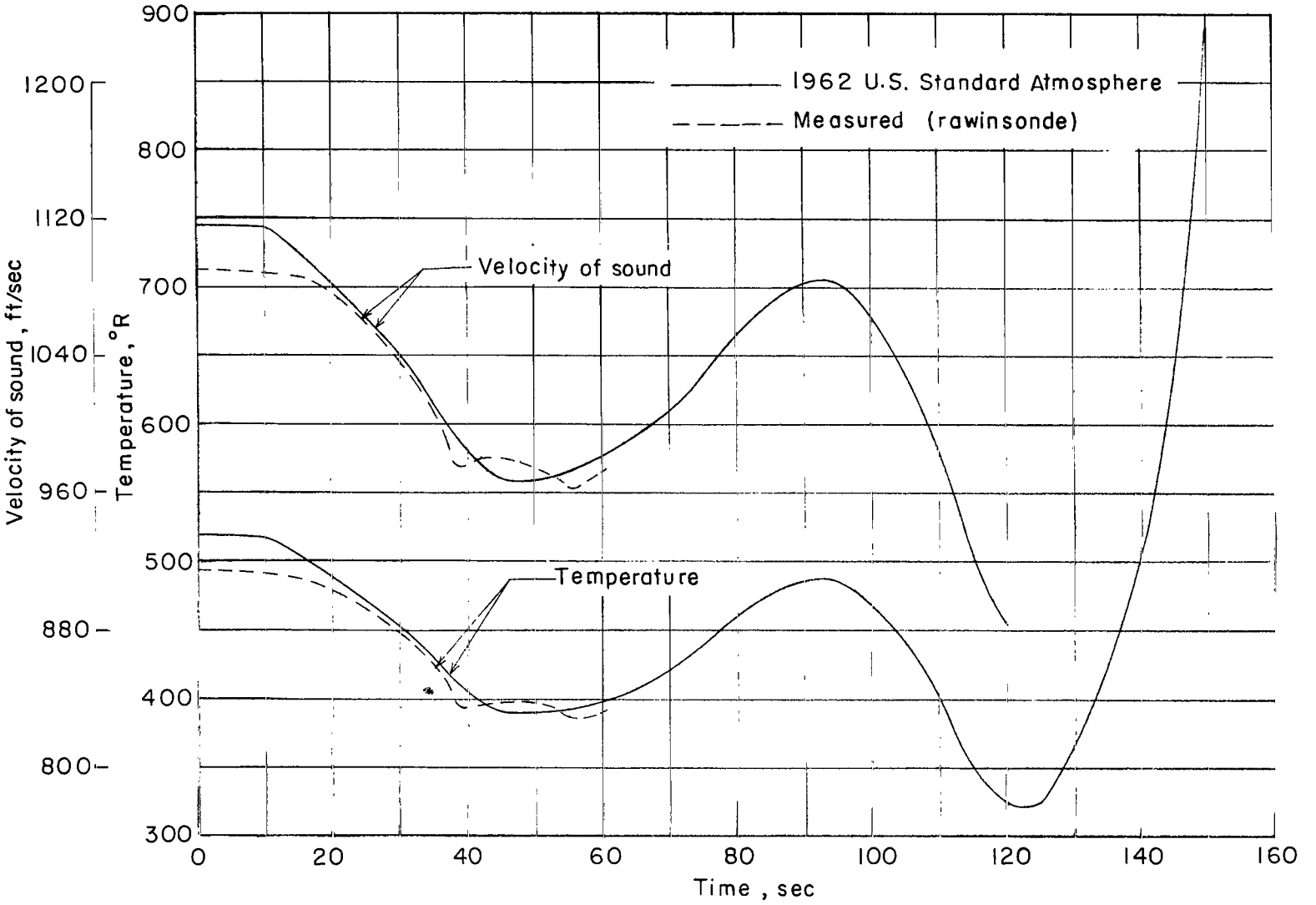

(a) Temperature and velocity of sound.

Figure 5.- Atmospheric conditions for Scout 115 flight test.

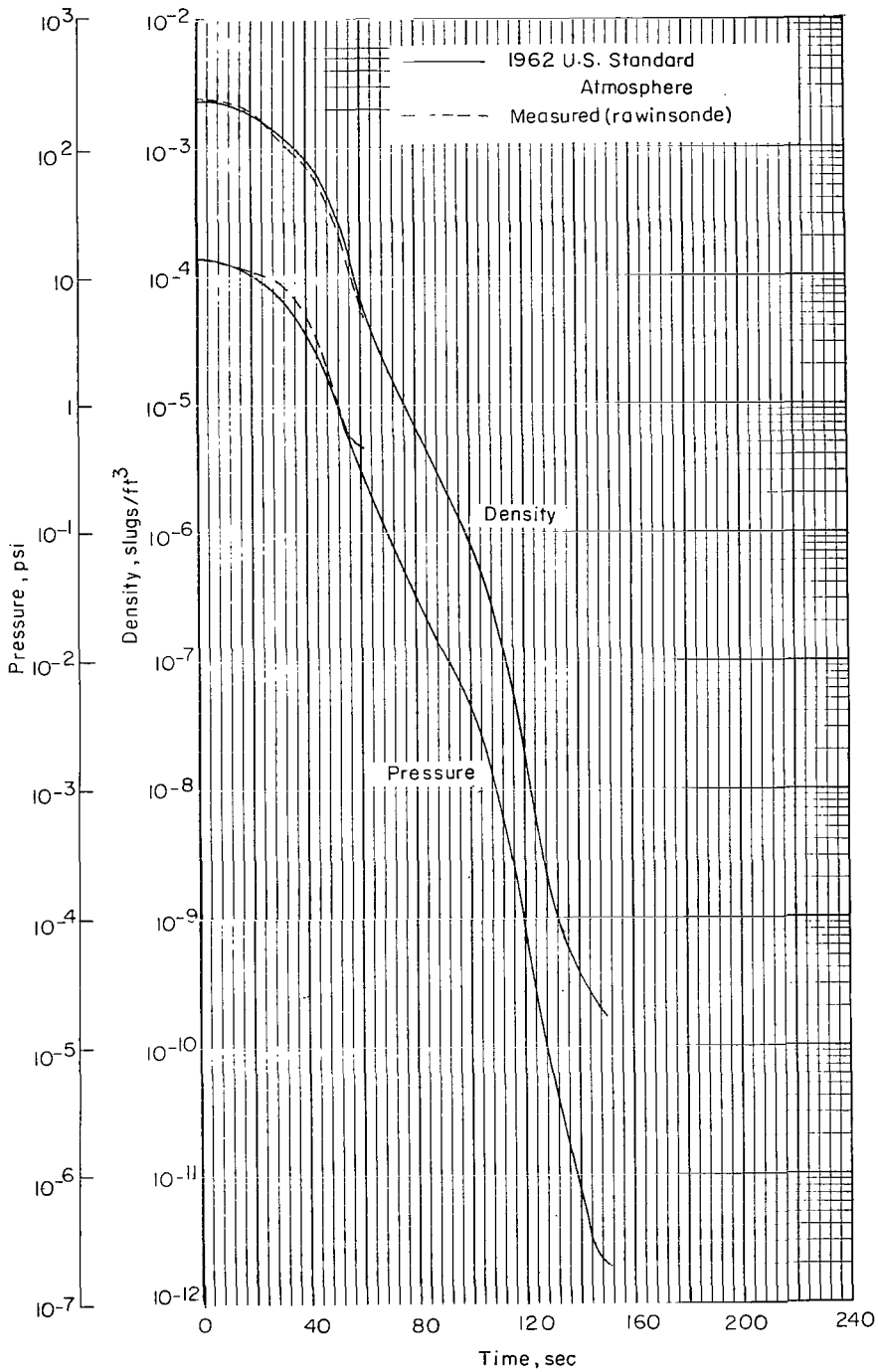

(b) Pressure and density.

Figure 5.- Concluded.

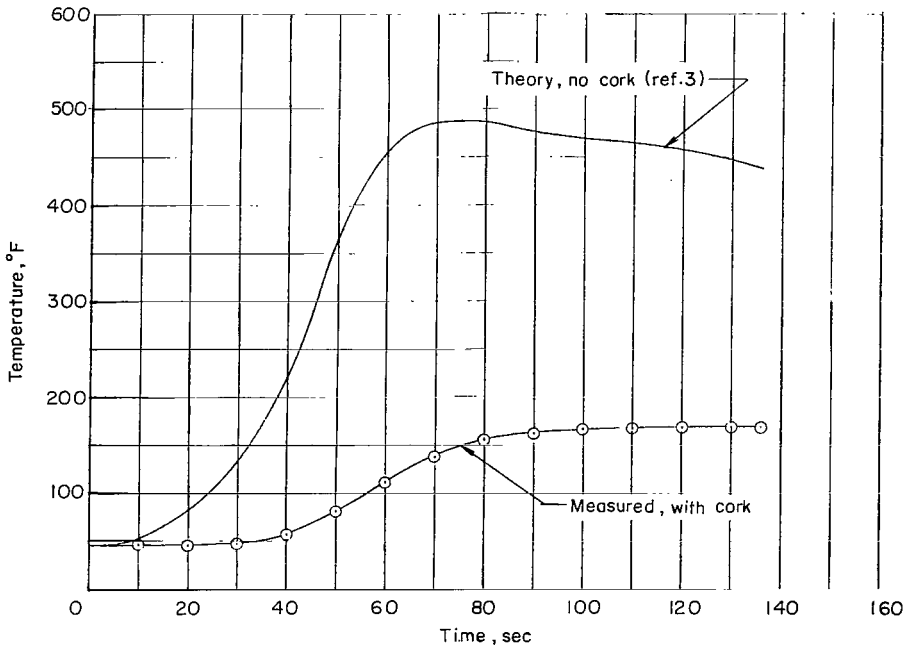

(a) Transition D section inside-surface temperatures with and without cork.

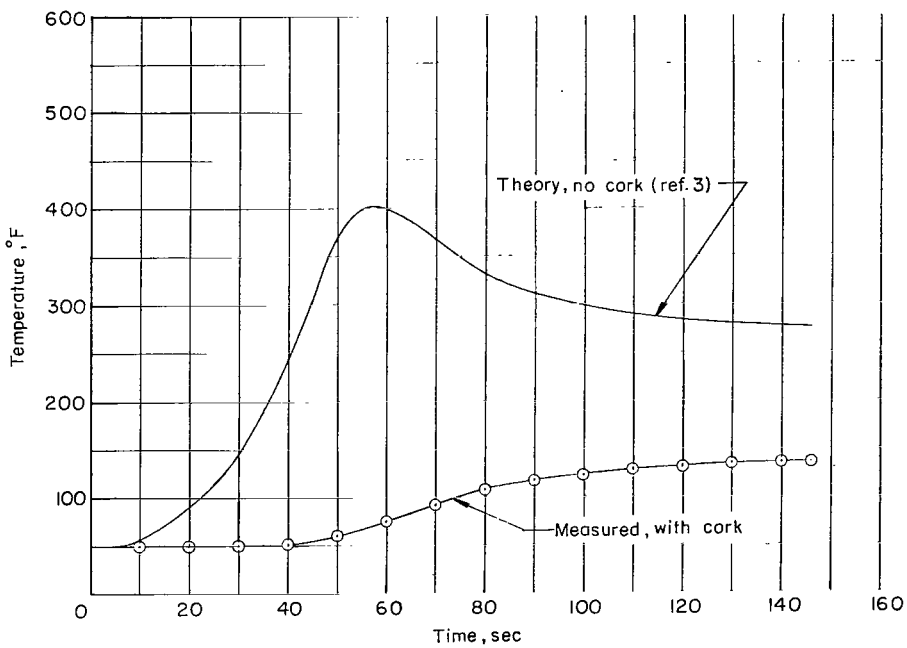

(b) Transition C section outside-surface temperatures with and without cork.

Figure 6.- Temperature histories for Scout 115, both with and without cork patch.

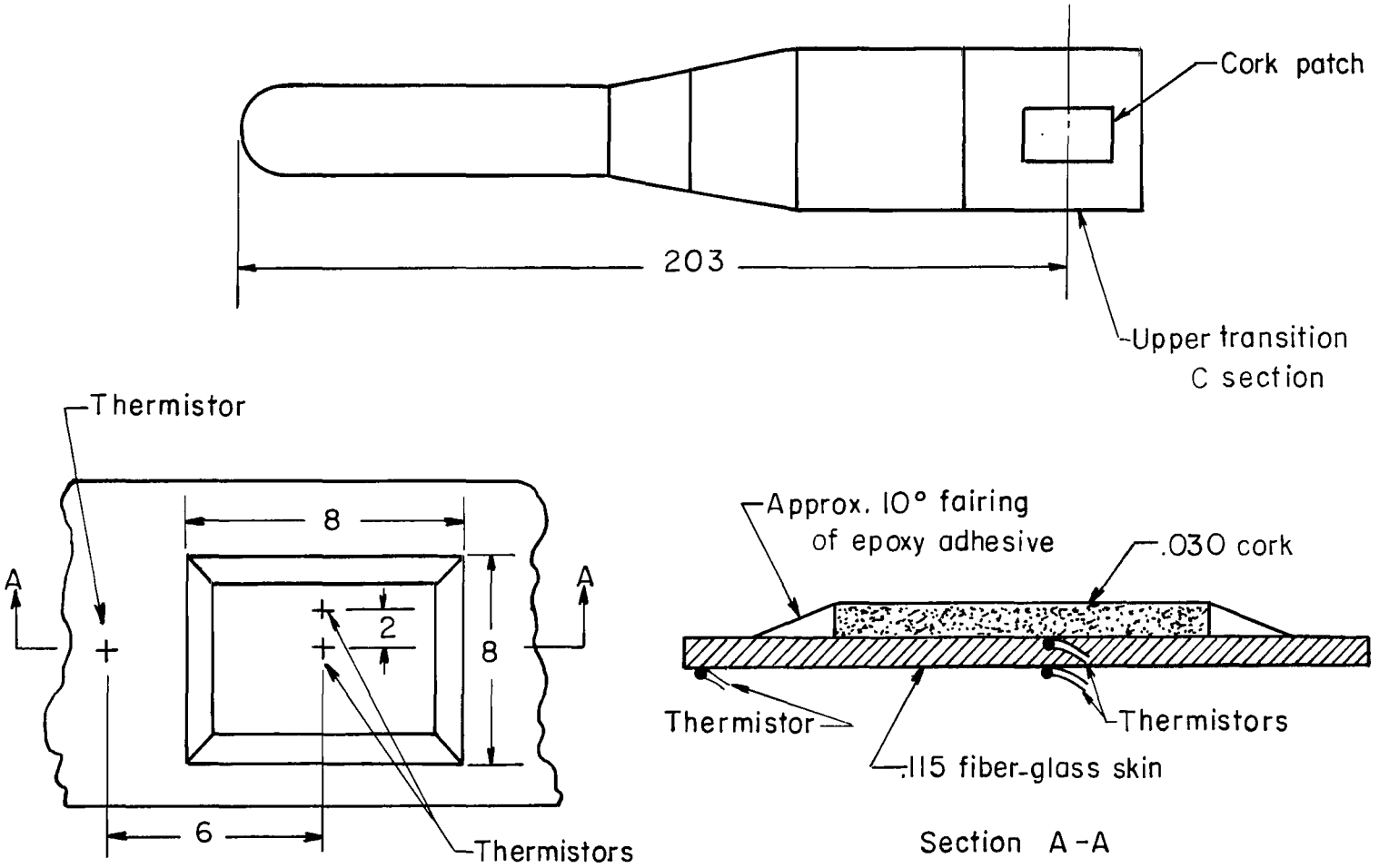

Figure 7.- Cork-patch installation on upper transition C section of Scout 116.
(All dimensions are in inches unless otherwise indicated.)

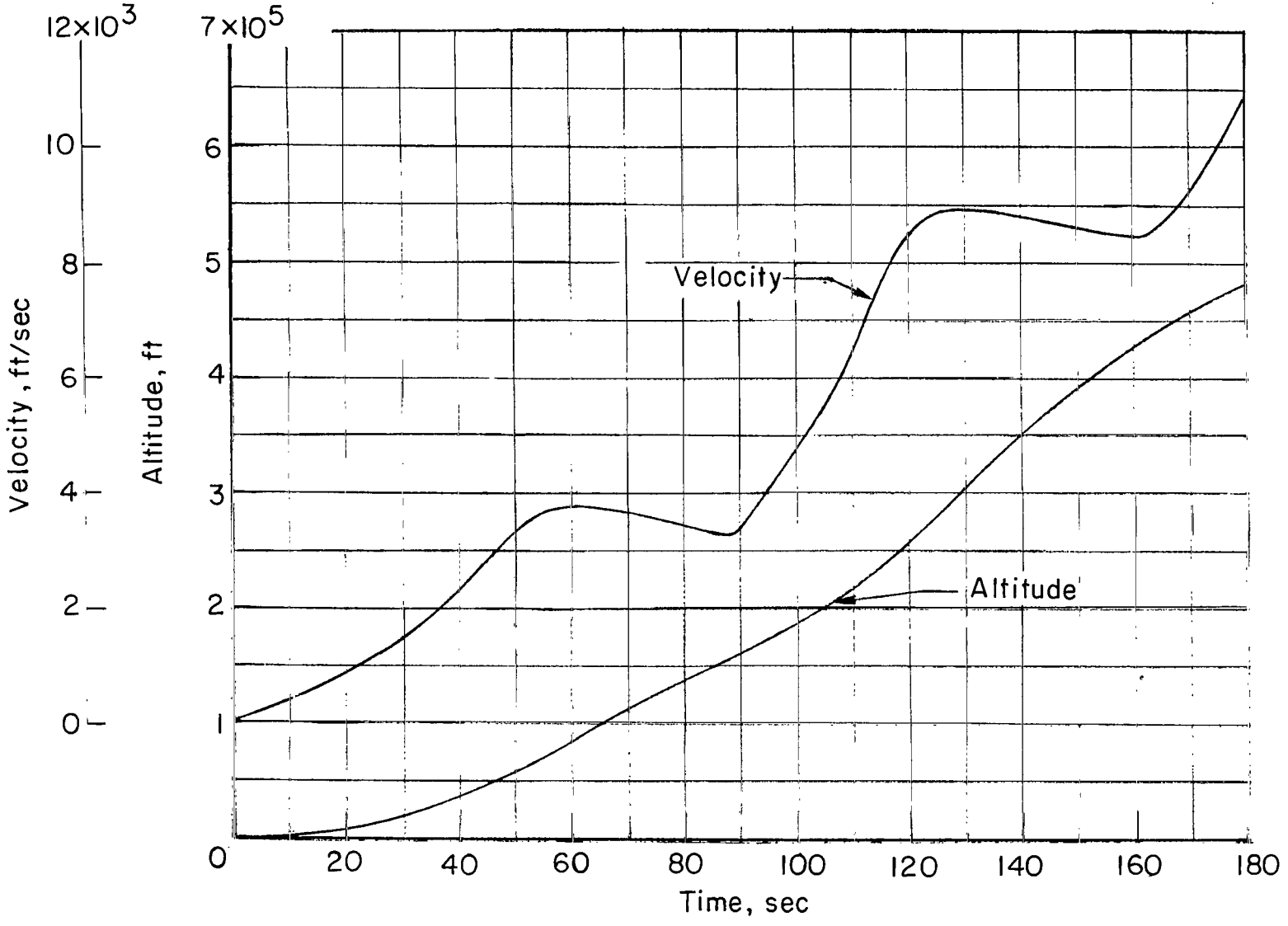

Figure 8.- Velocity and altitude histories for Scout 116 flight test.

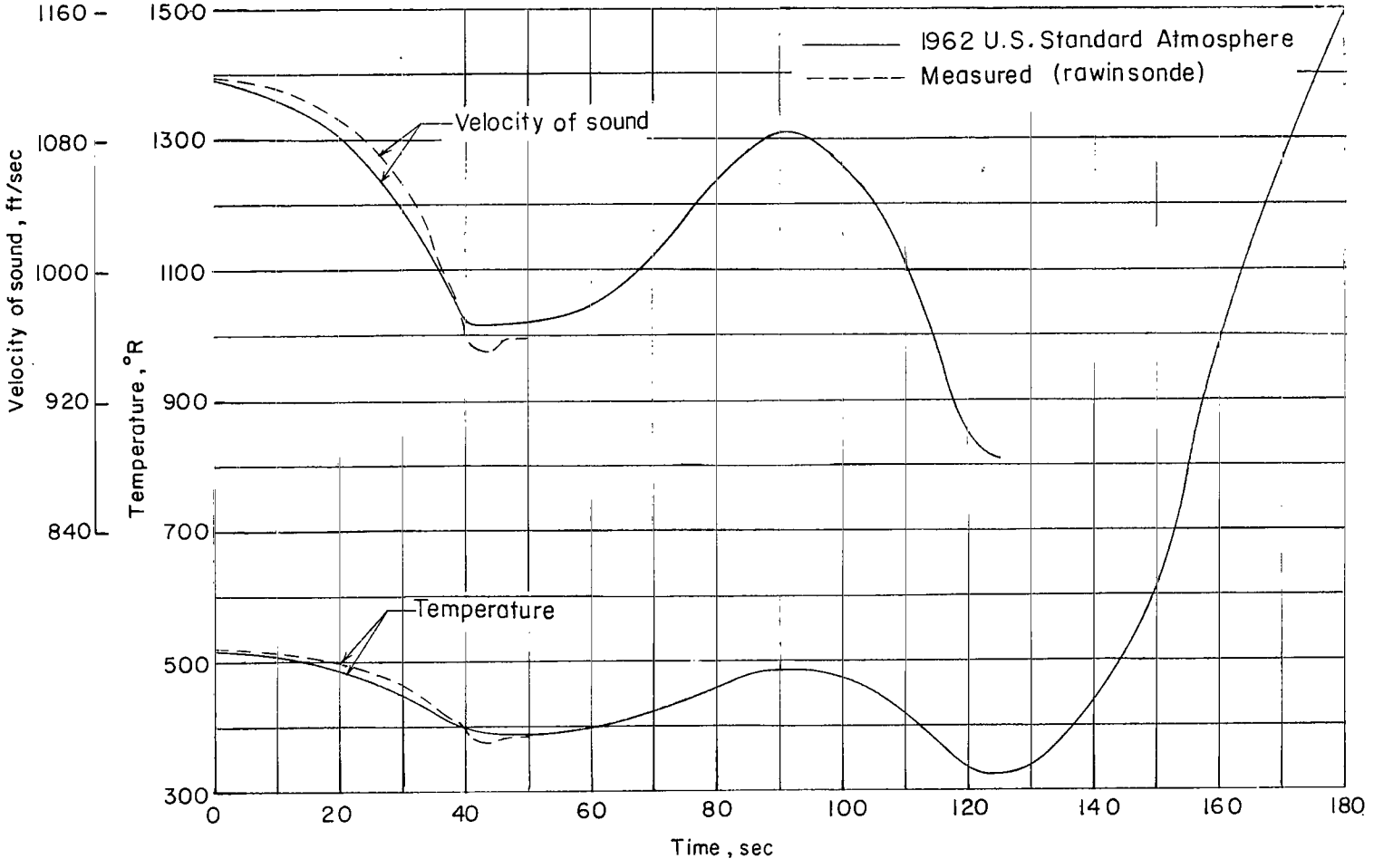

(a) Temperature and velocity of sound.

Figure 9.- Atmospheric conditions for Scout 116 flight test.

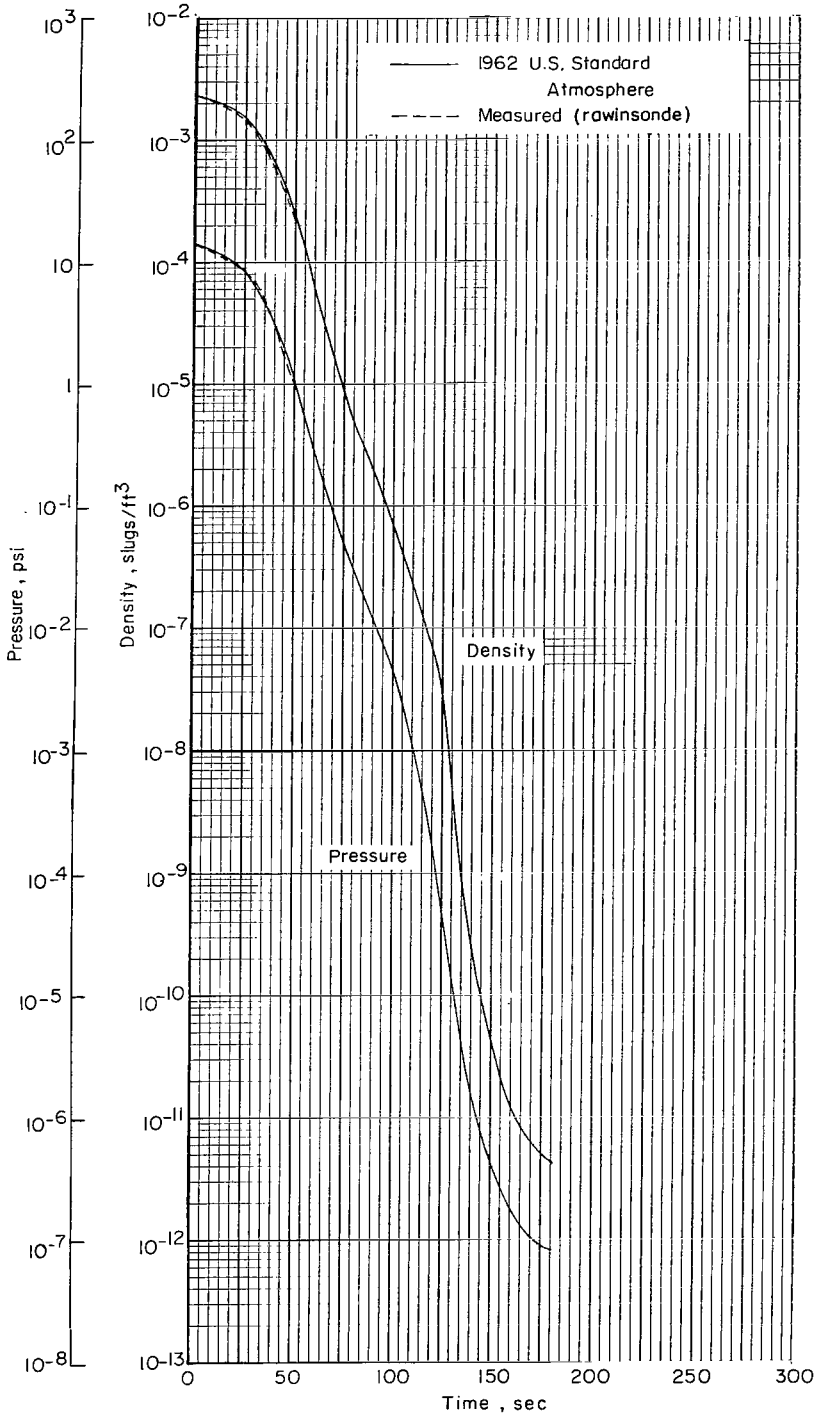

(b) Pressure and density.

Figure 9.- Concluded

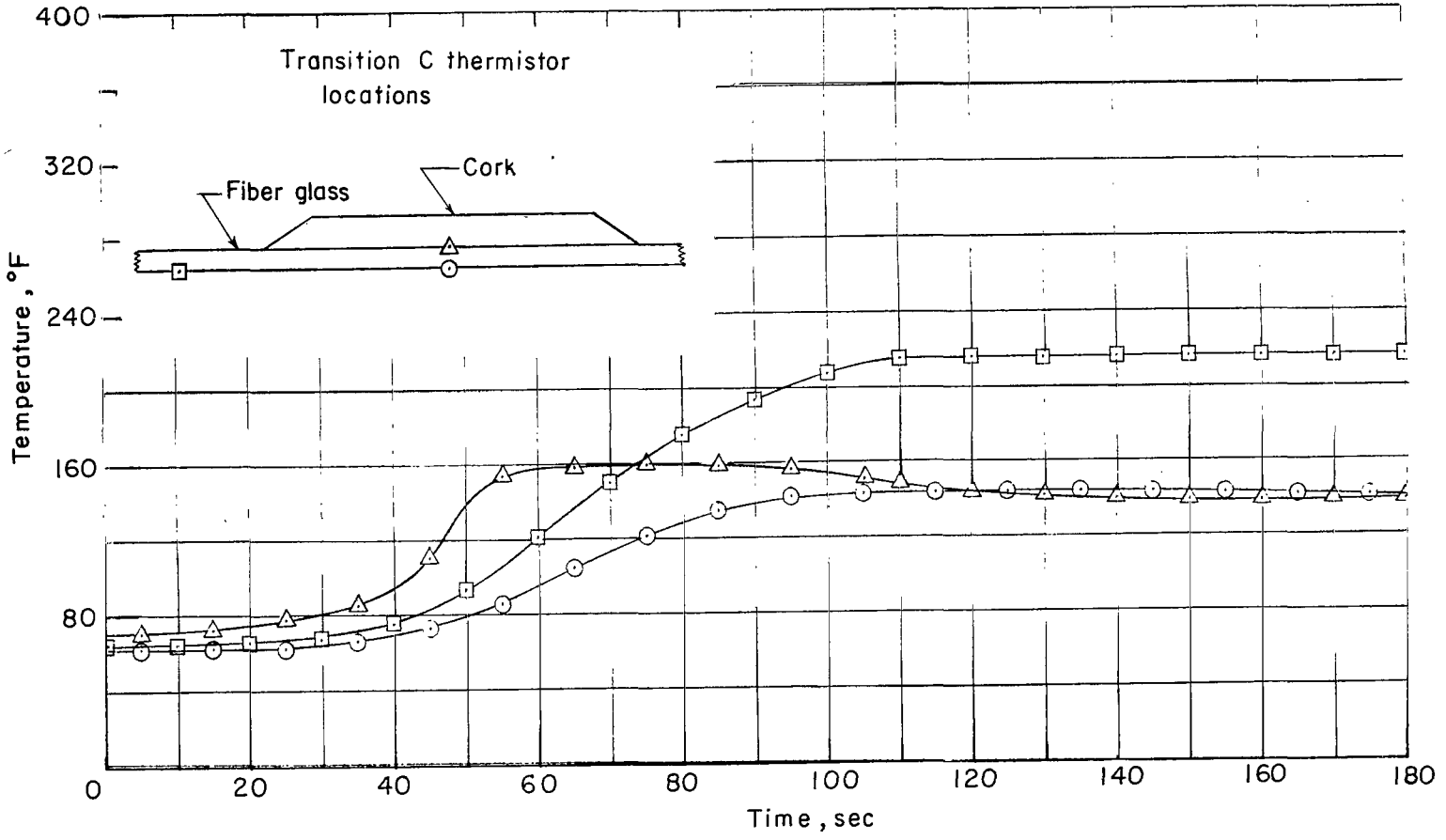

Figure 10.- Thermistor installations and temperature histories for Scout 116 flight test.

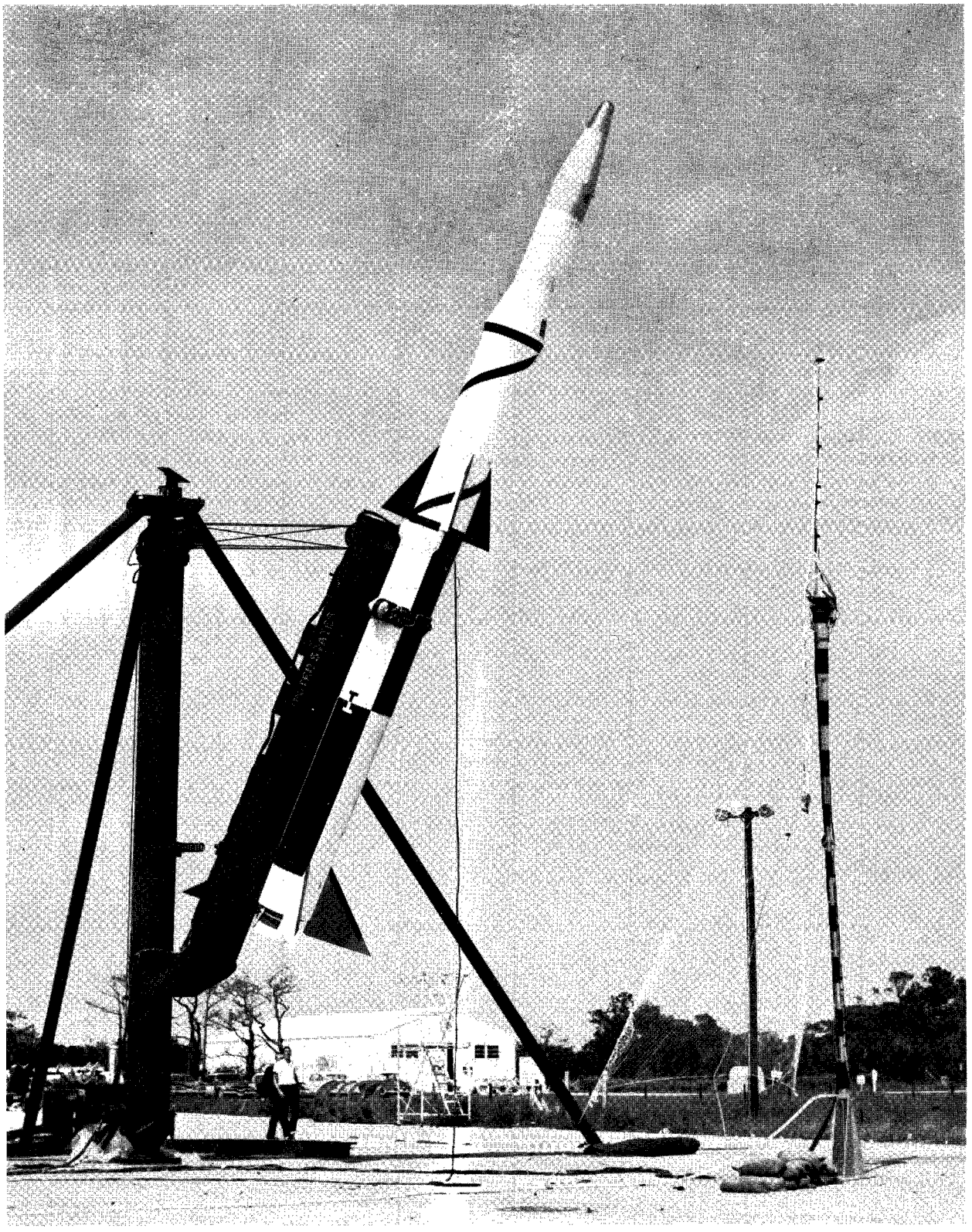

Figure 11.- RAM B vehicle. L-62-7685

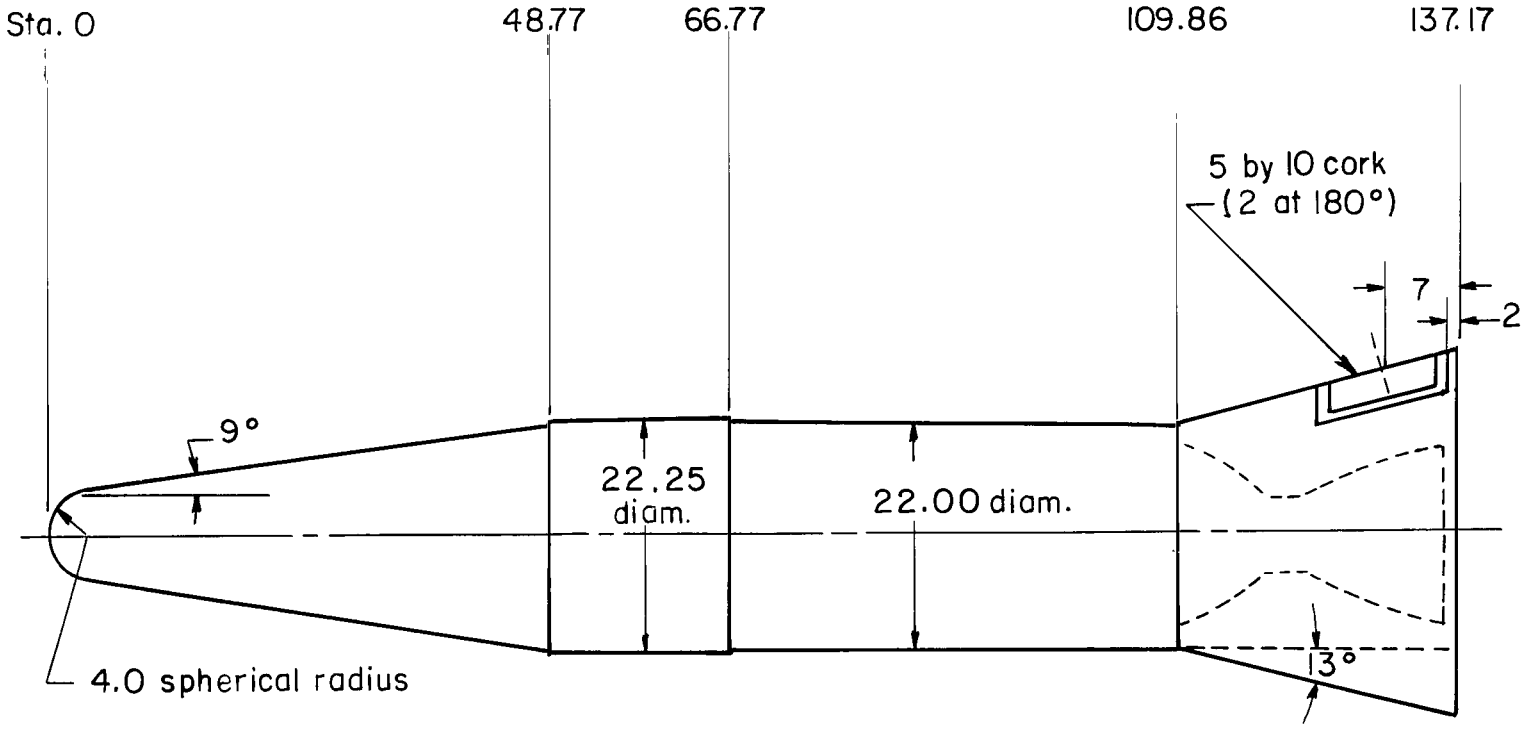

Figure 12.- Sketch of RAM B1 vehicle third stage with cork locations shown.
(All dimensions are in inches unless otherwise indicated.)

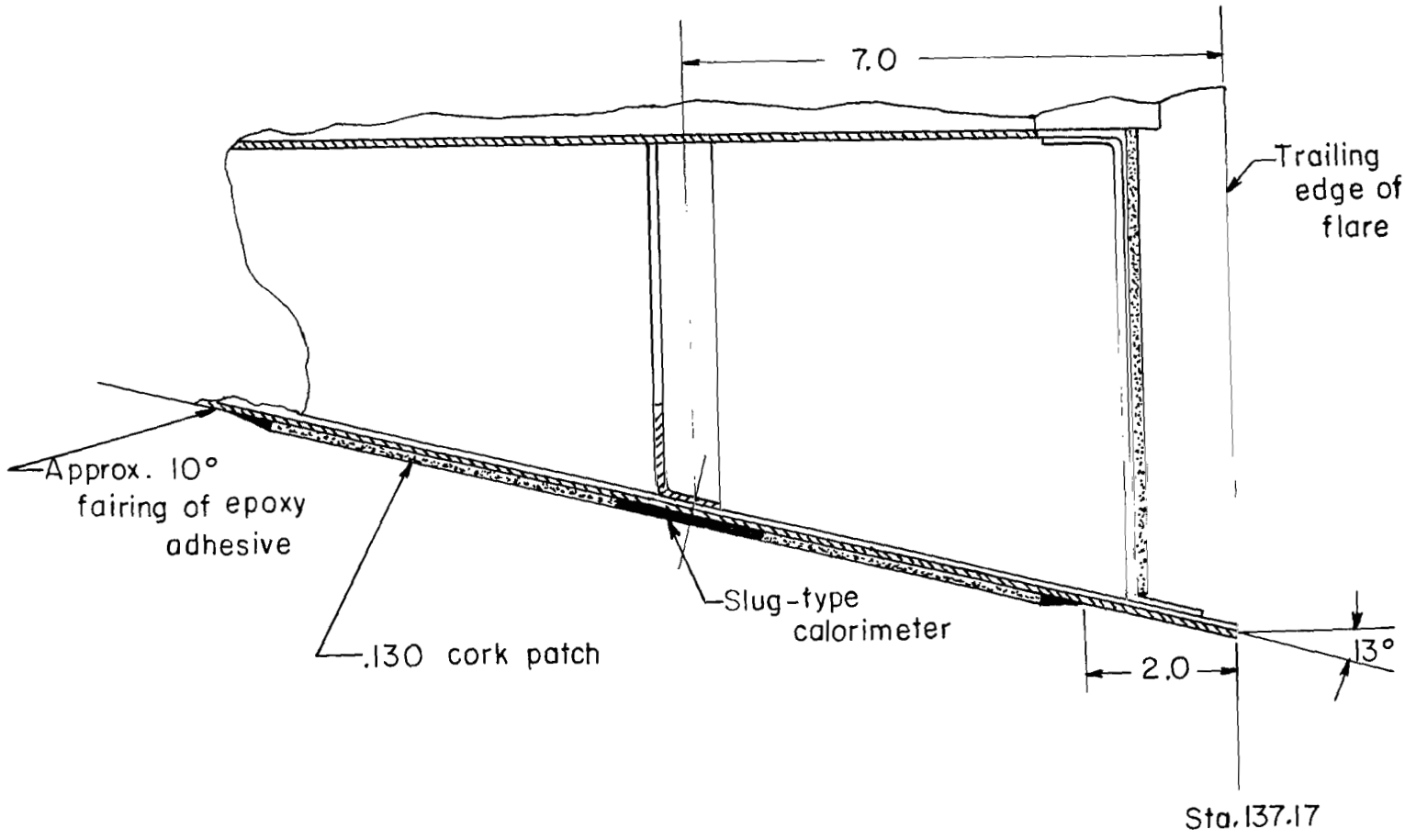

Figure 13.- Calorimeter installation on RAM B1 third-stage flare.
(All dimensions are in inches unless otherwise indicated.)

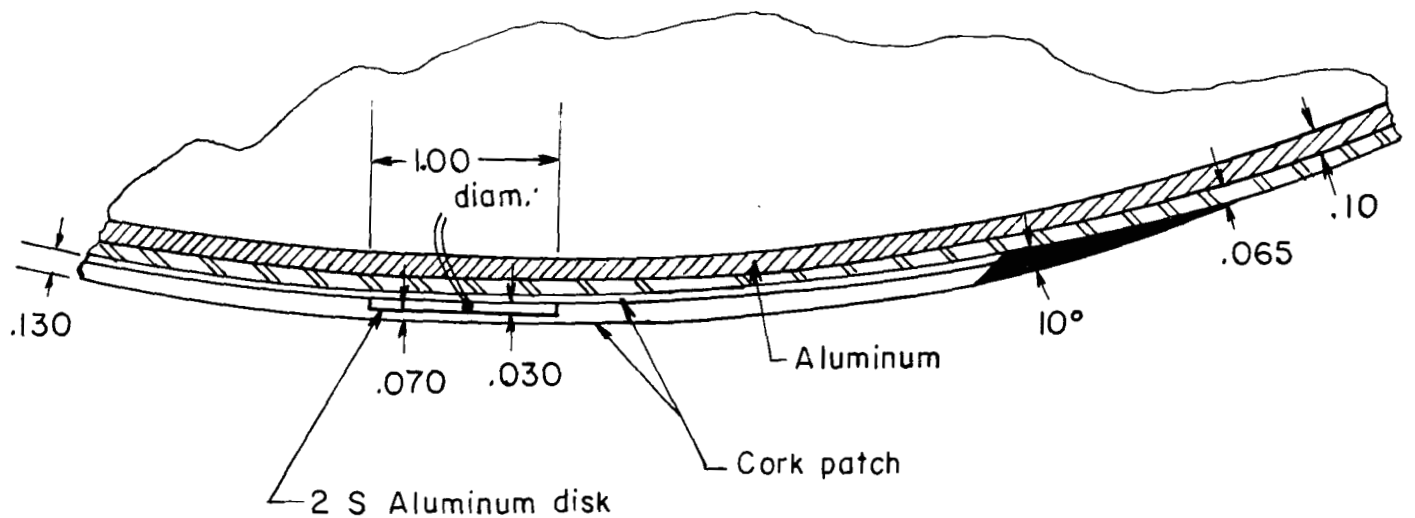

Figure 14.- Cross section of cork patch showing thermocouple assembly on RAM B1.
(All dimensions are in inches unless otherwise indicated.)

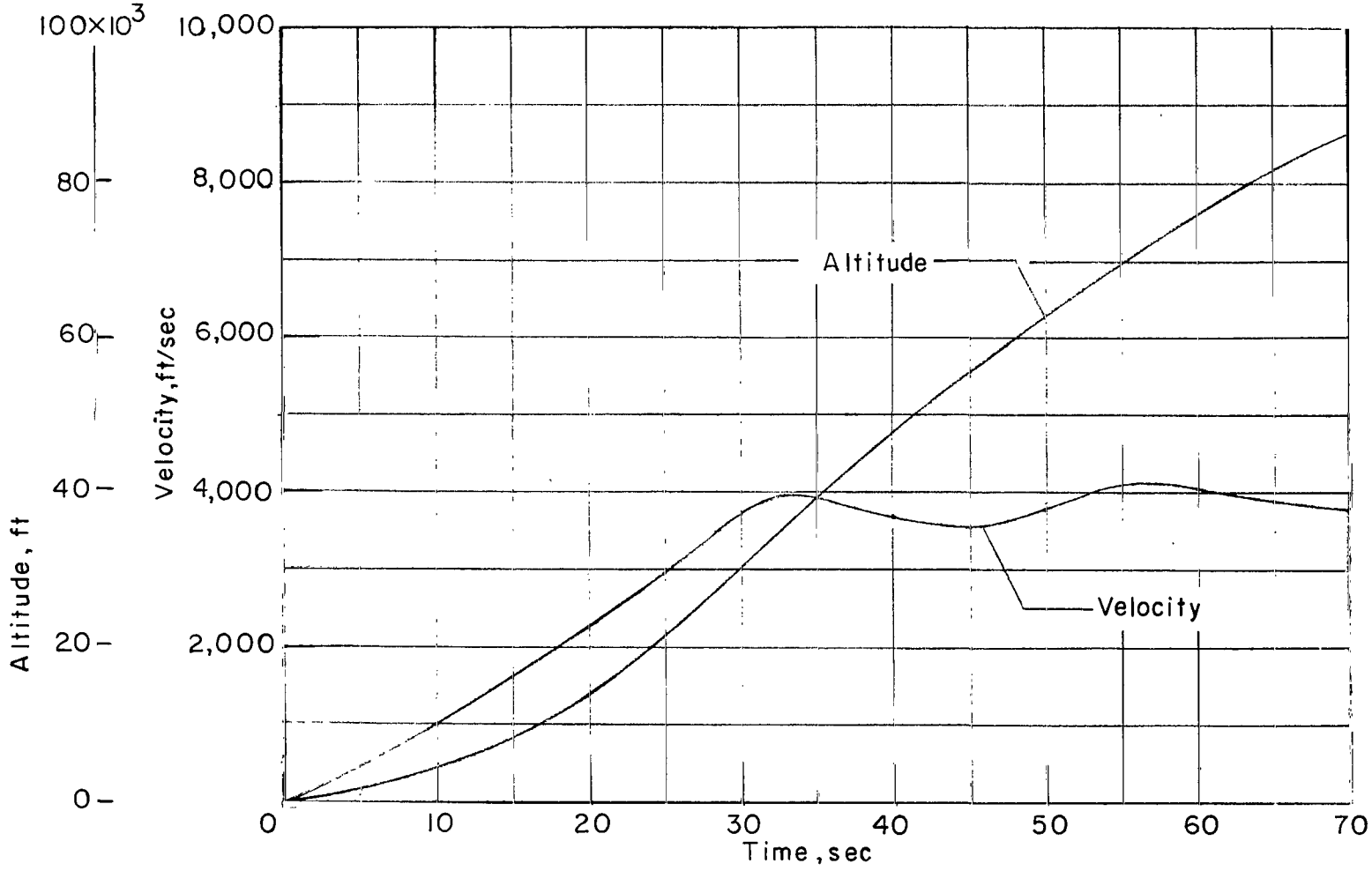

Figure 15.- Altitude and velocity histories of the RAM B1 vehicle.

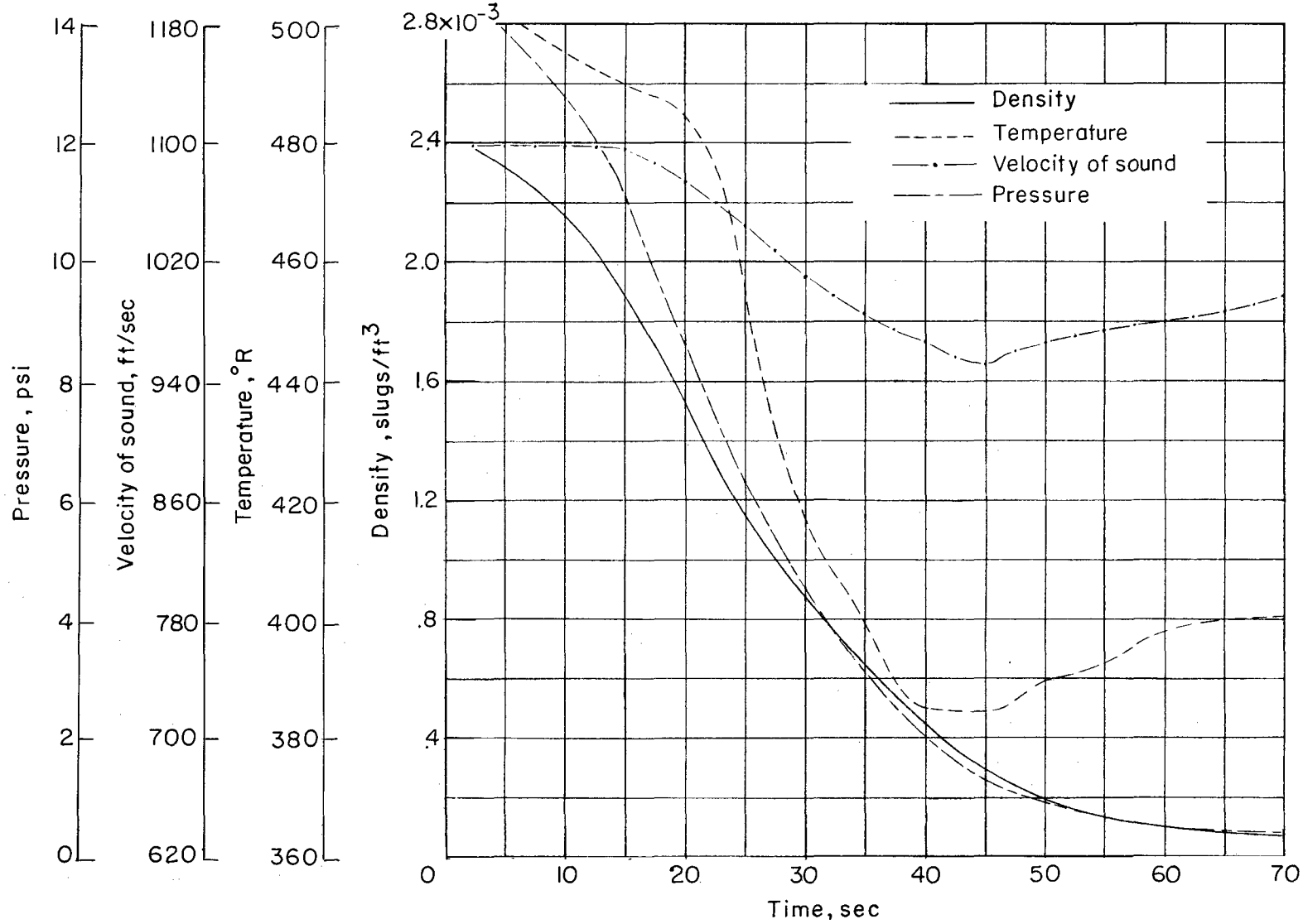

Figure 16.- Measured atmospheric conditions for RAM B1 flight.

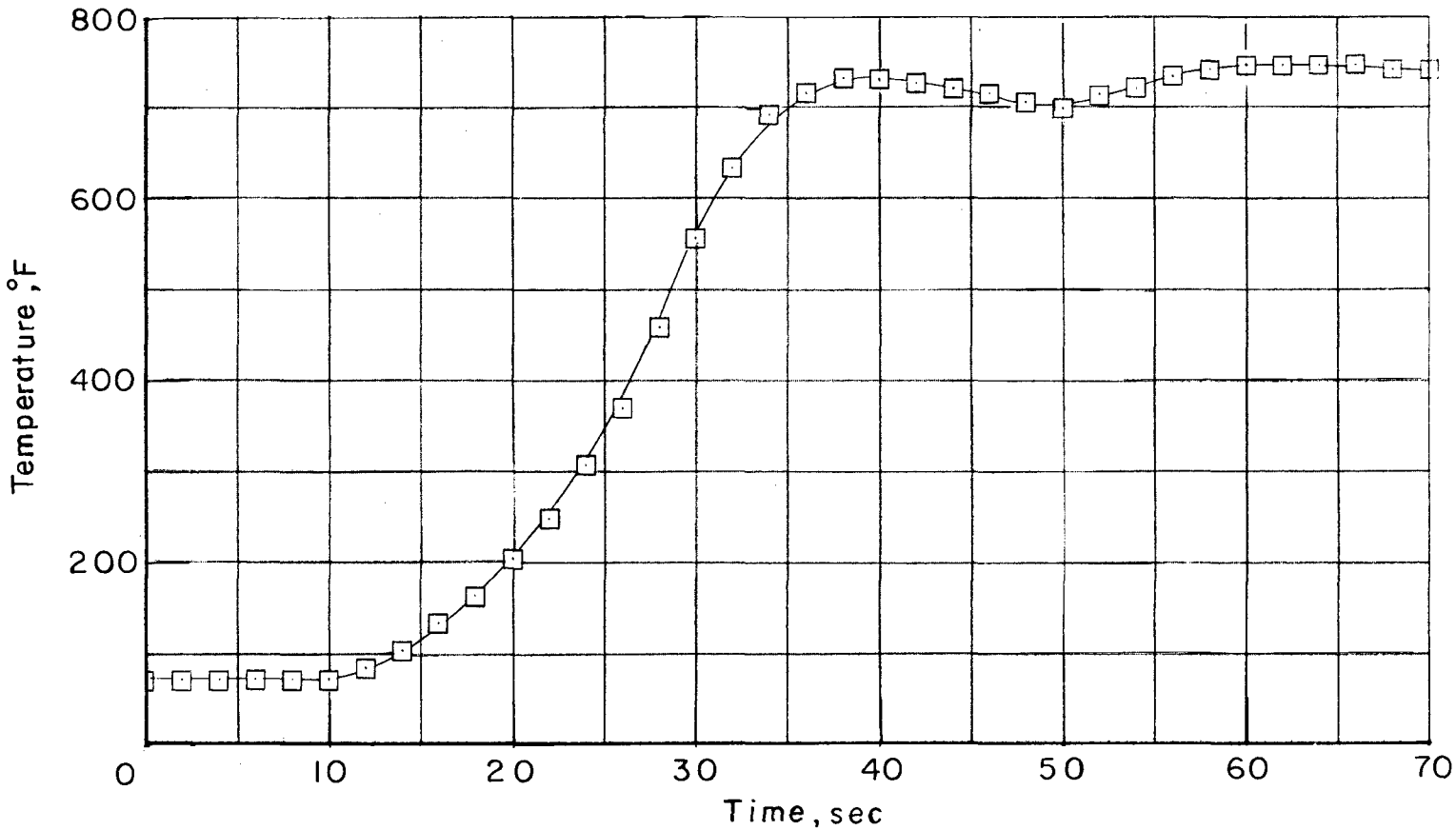

Figure 17.- Temperature history of RAM B1 calorimeter.

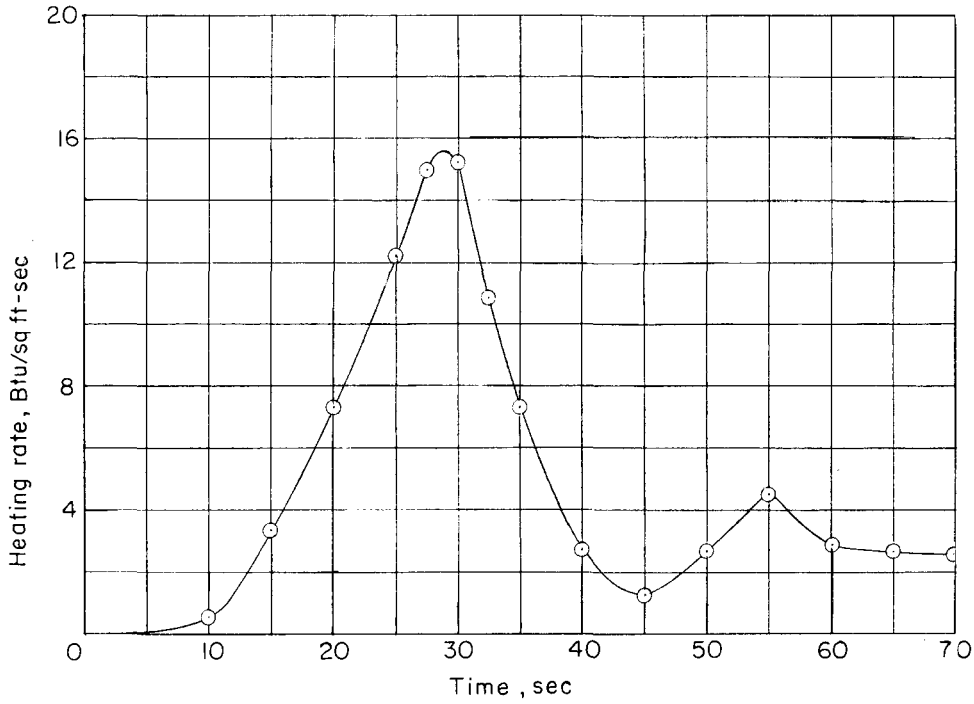

(a) Heating rate obtained from slug-type calorimeter.

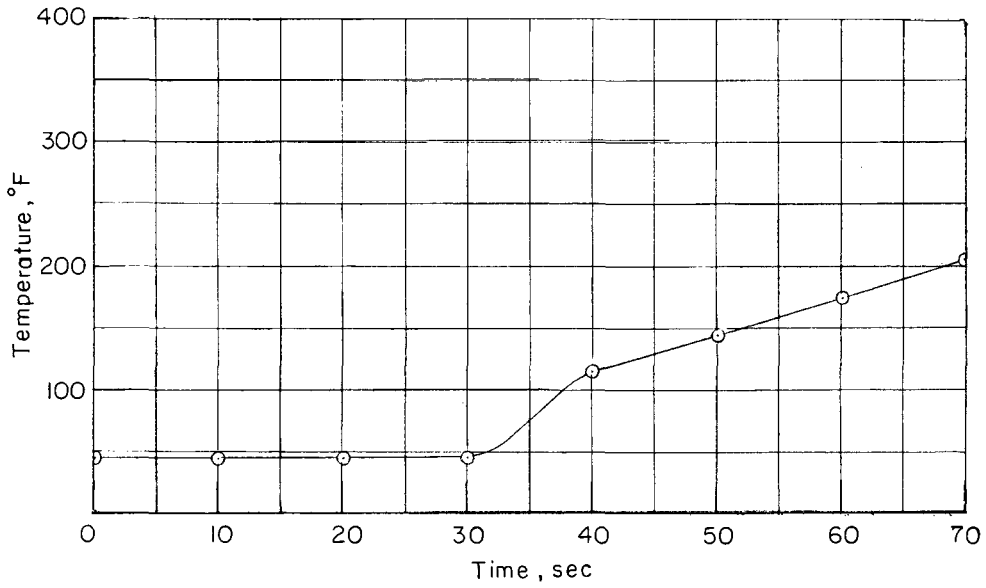

(b) Measured temperature for the thermocouple assembly.

Figure 18.- Heating-rate and temperature histories for RAM B1.

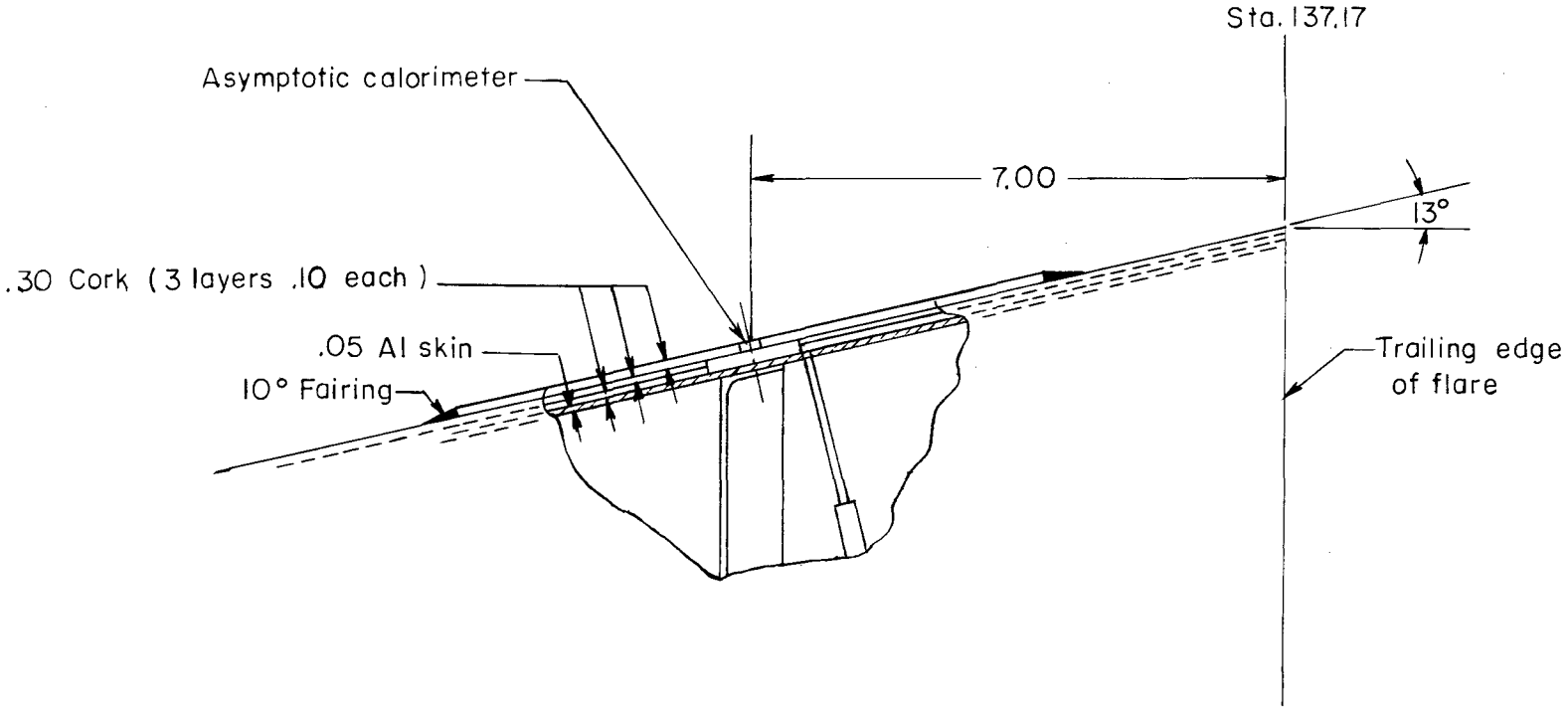

Figure 19.- Calorimeter installation on RAM B2 third-stage flare.
(All dimensions are in inches unless otherwise indicated.)

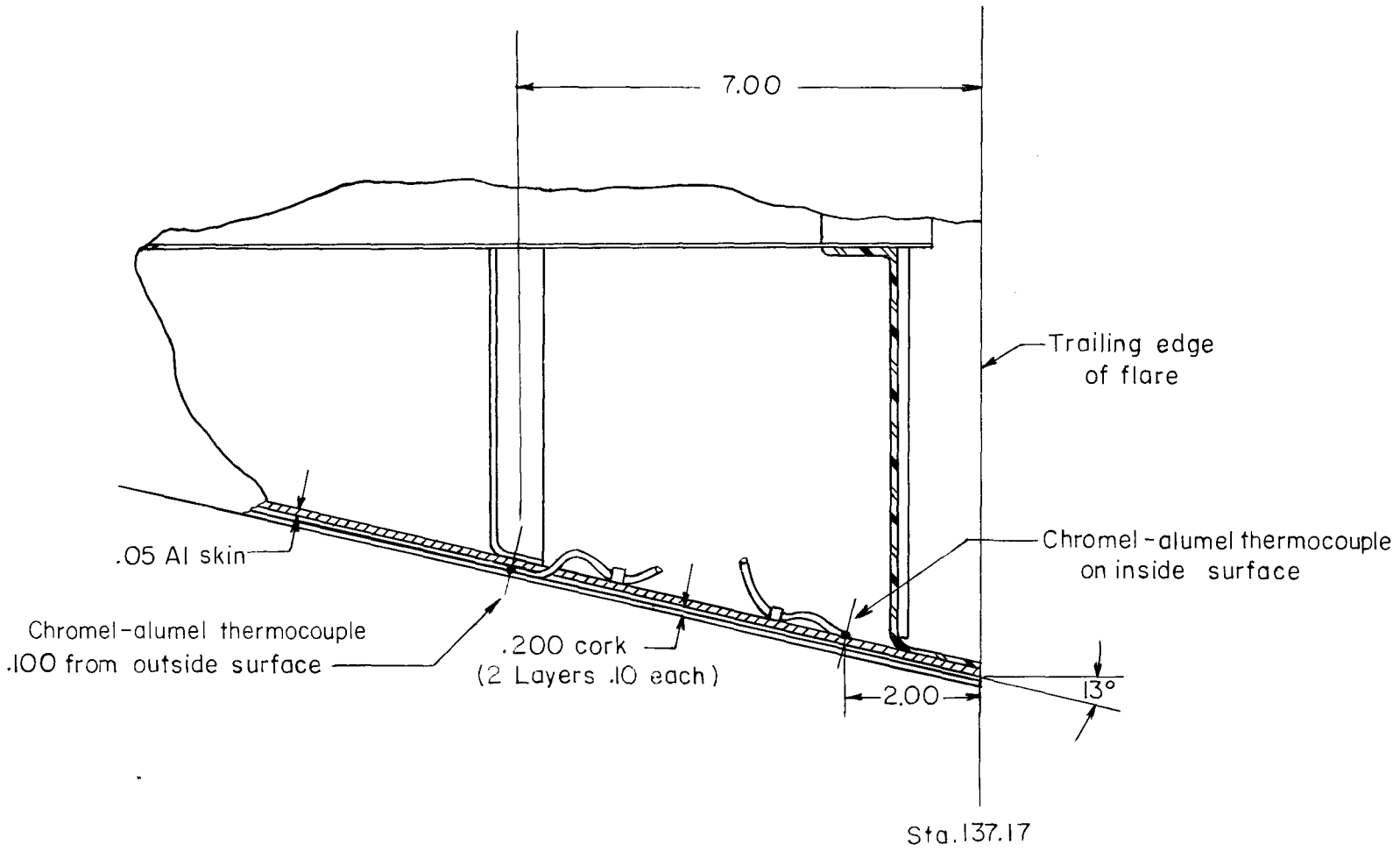

Figure 20.- Thermocouple installations on RAM B2 third-stage flare.
(All dimensions are in inches unless otherwise indicated.)

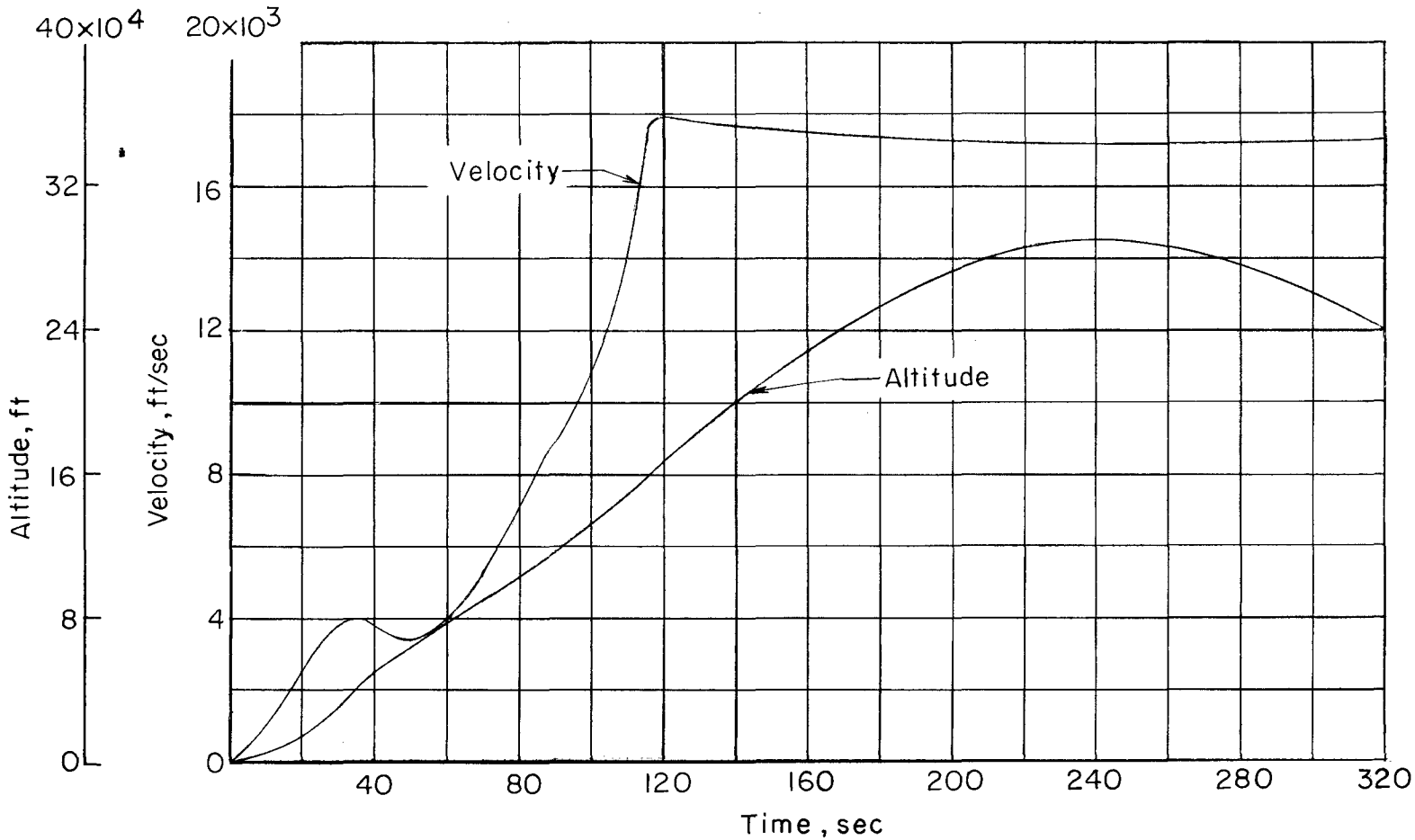

Figure 21.- Velocity and altitude histories for RAM B2 flight test.

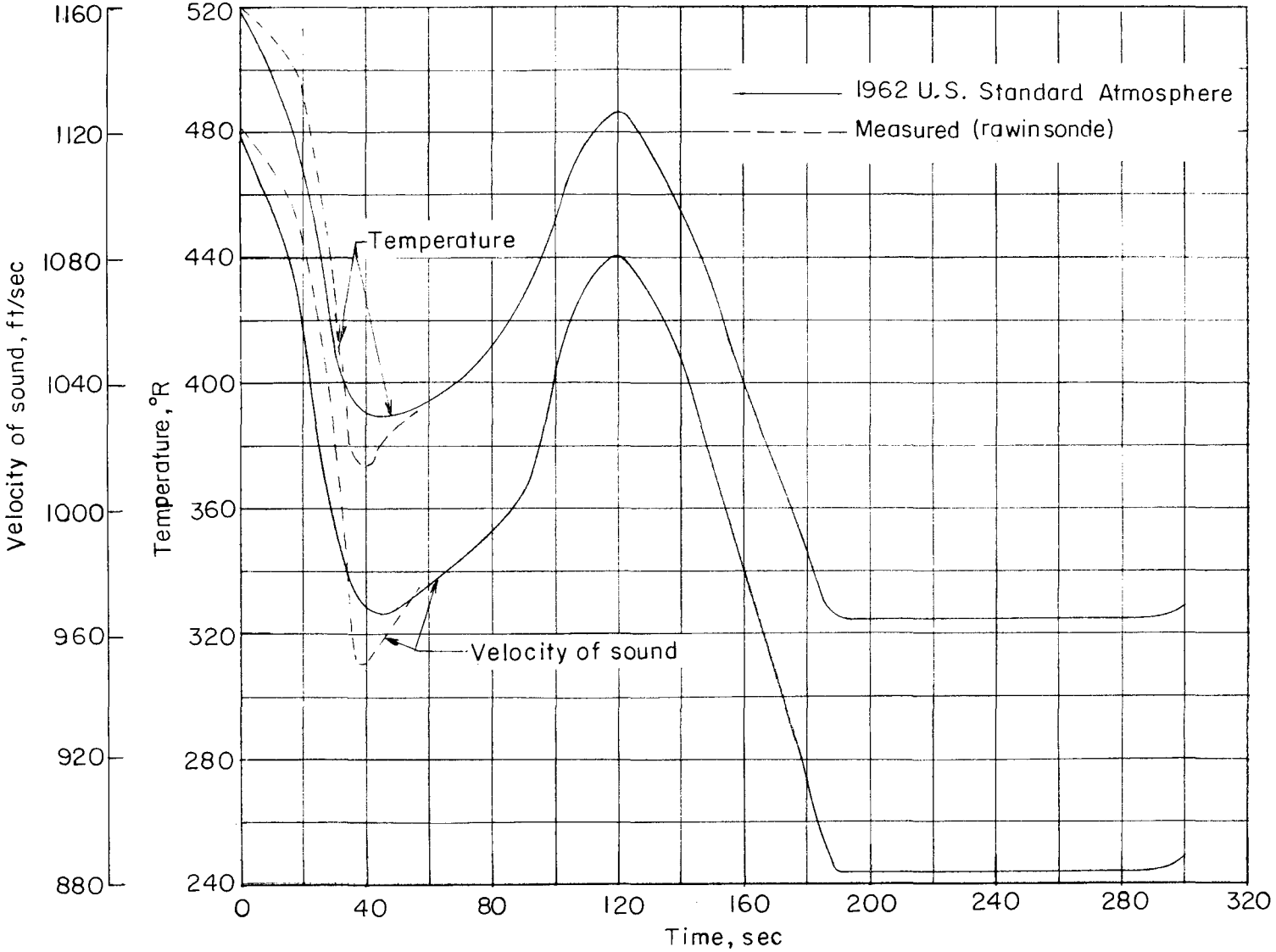

(a) Temperature and velocity of sound.

Figure 22.- Atmospheric conditions for RAM B2 flight test.

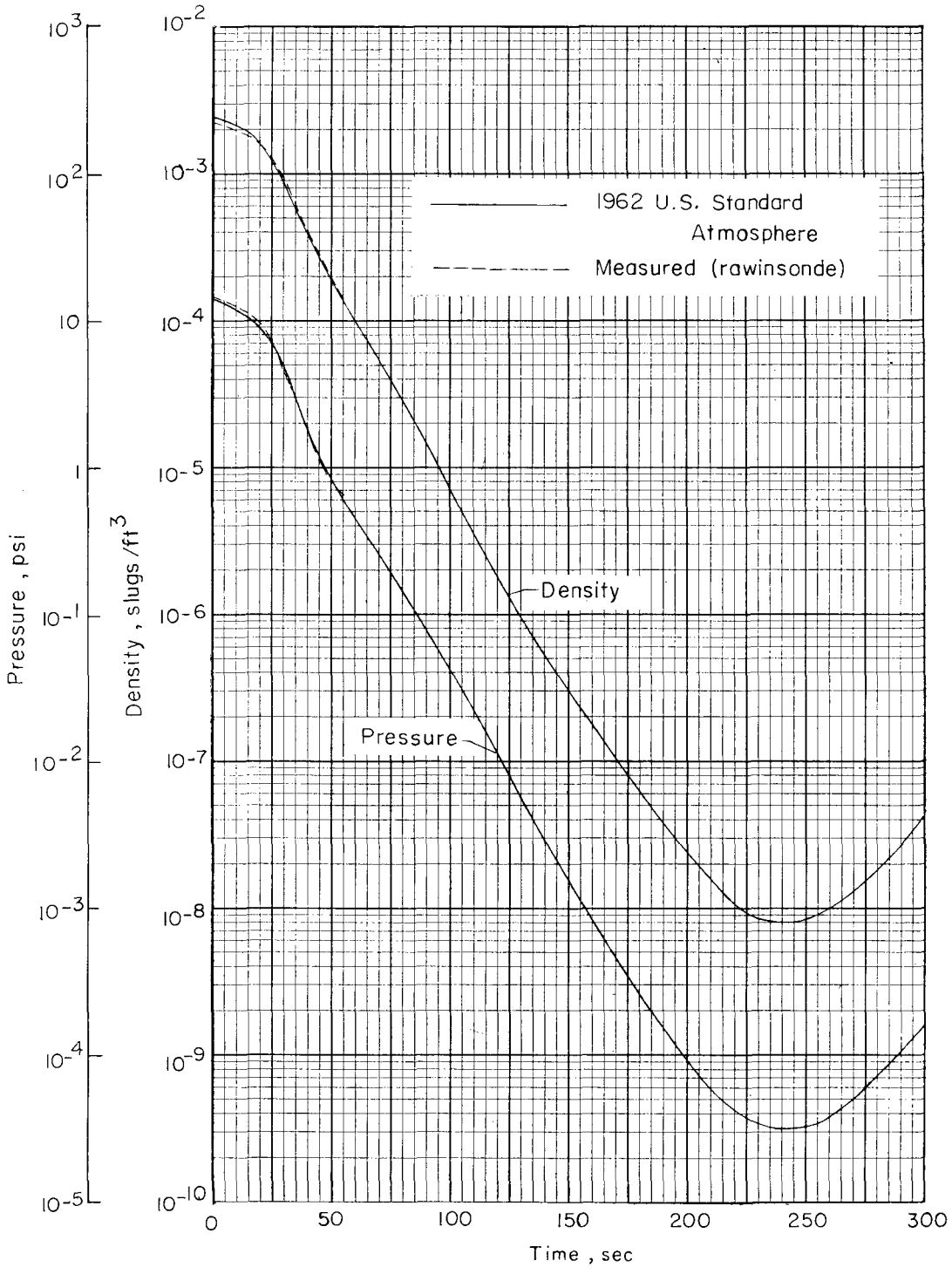

(b) Pressure and density.

Figure 22.- Concluded.

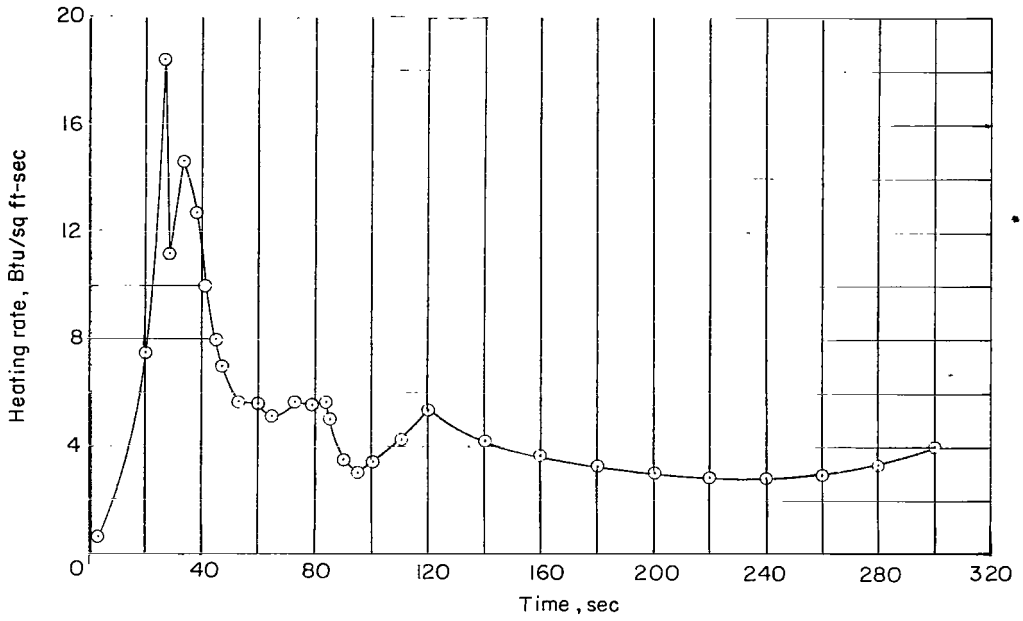

(a) Heating rate obtained from asymptotic calorimeter.

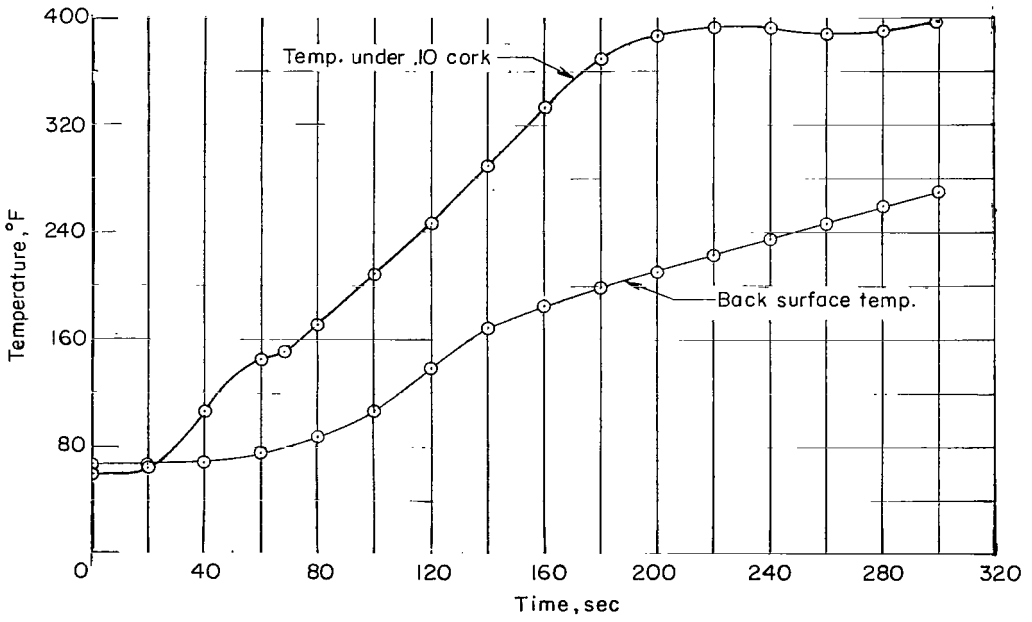

(b) Measured temperature for two locations under cork.

Figure 23.- Heating-rate and temperature histories for RAM B2.

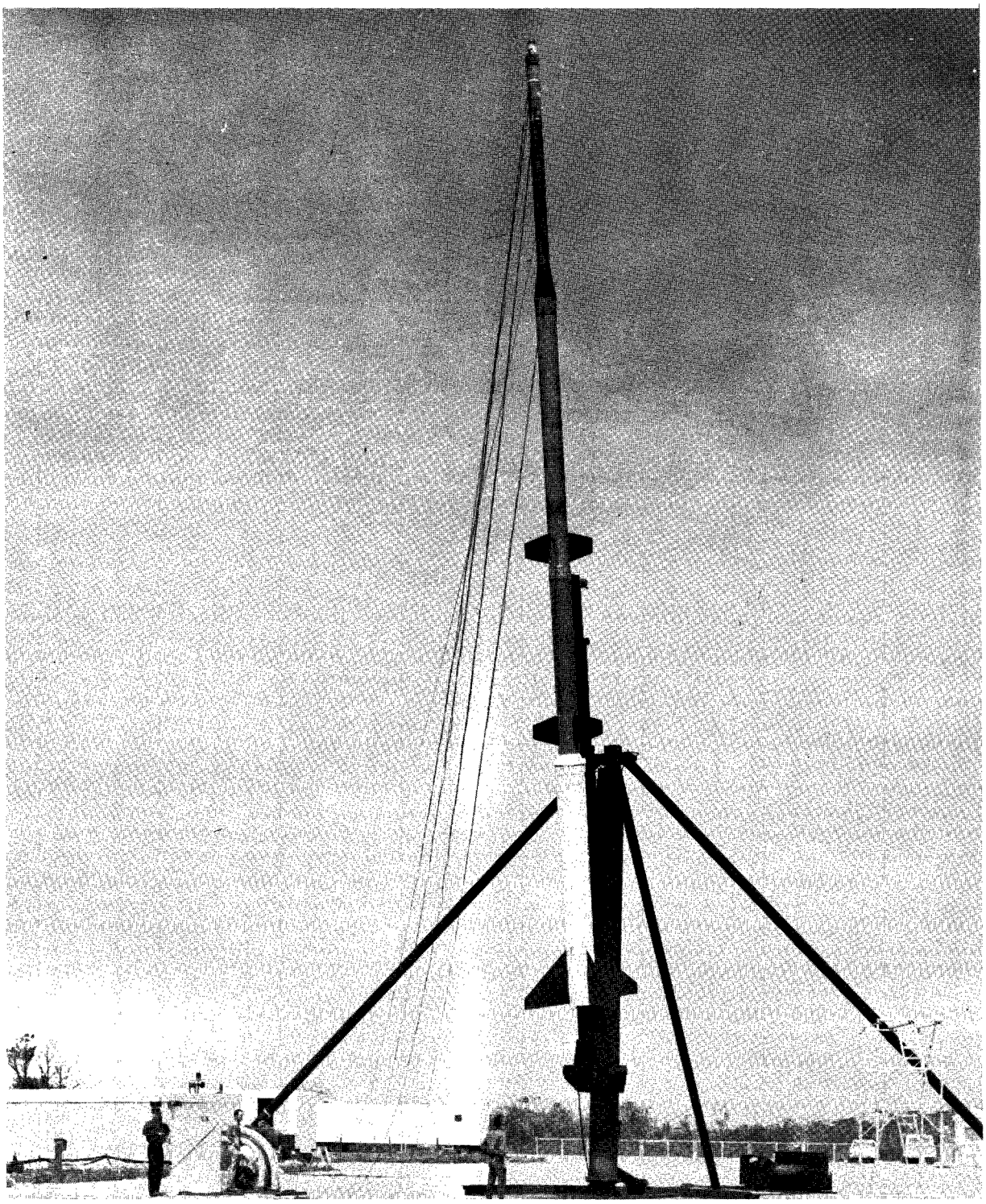

Figure 24.- Four-stage payload recovery vehicle. L-63-4946

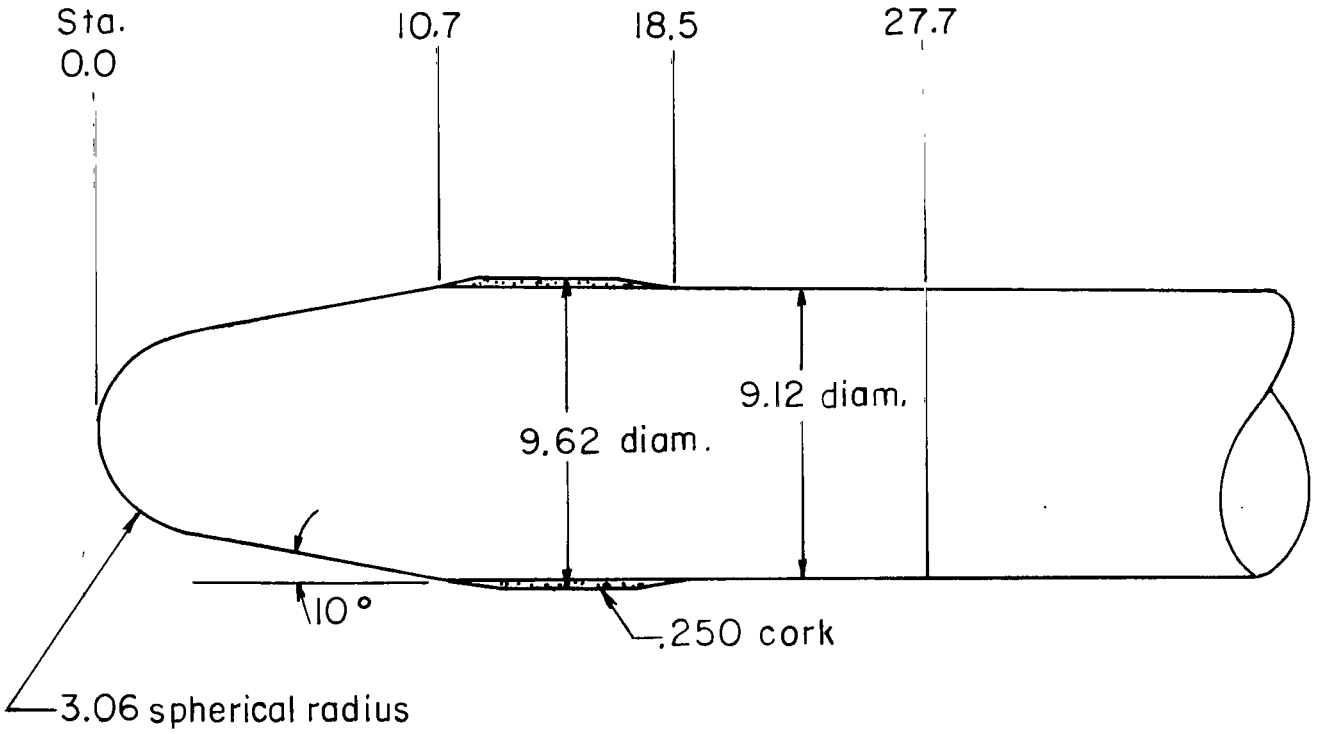

Figure 25.- Sketch showing cork location on recoverable payload.
(All dimensions are in inches unless otherwise indicated.)

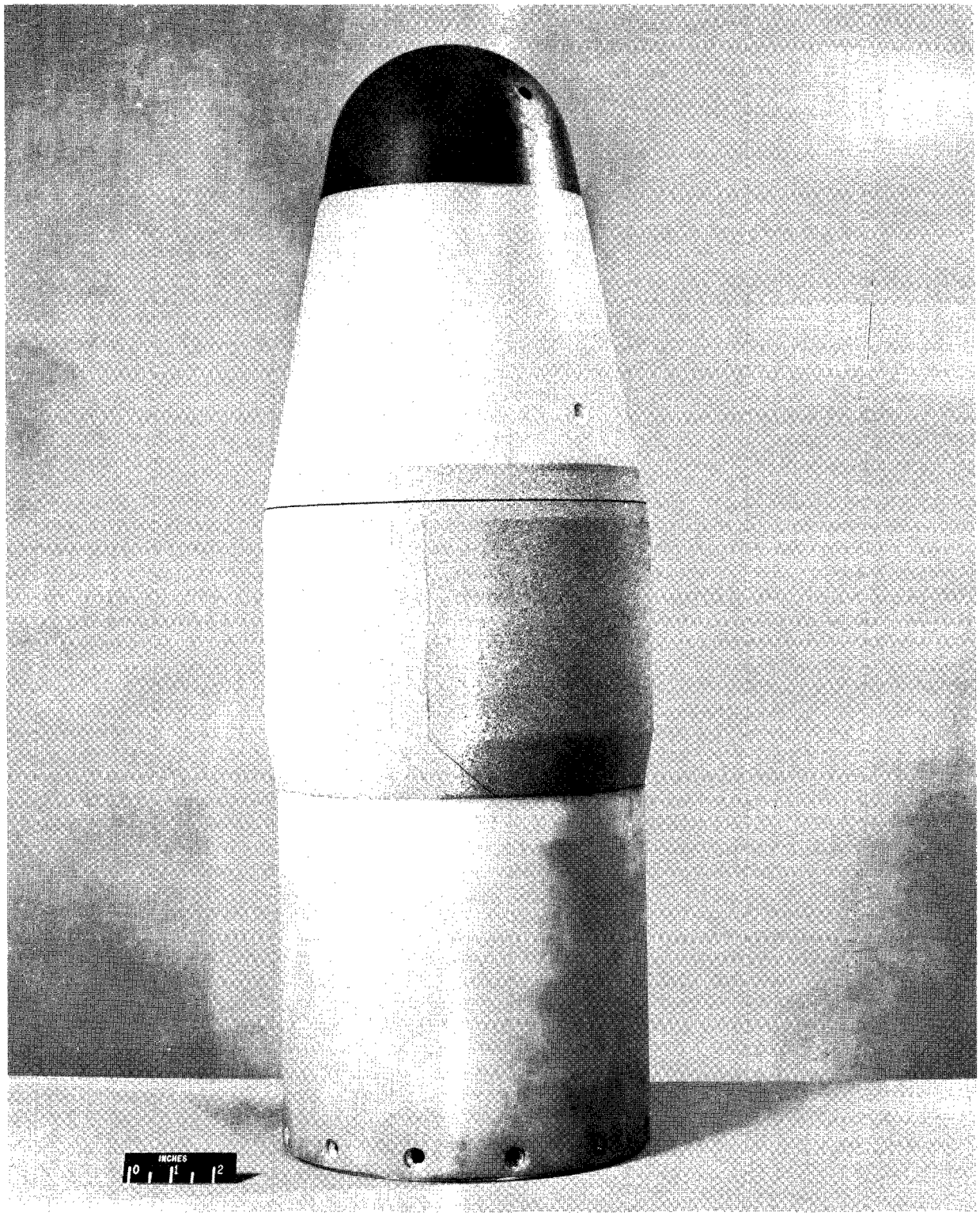

Figure 26.- Recoverable payload before flight. L-63-3334

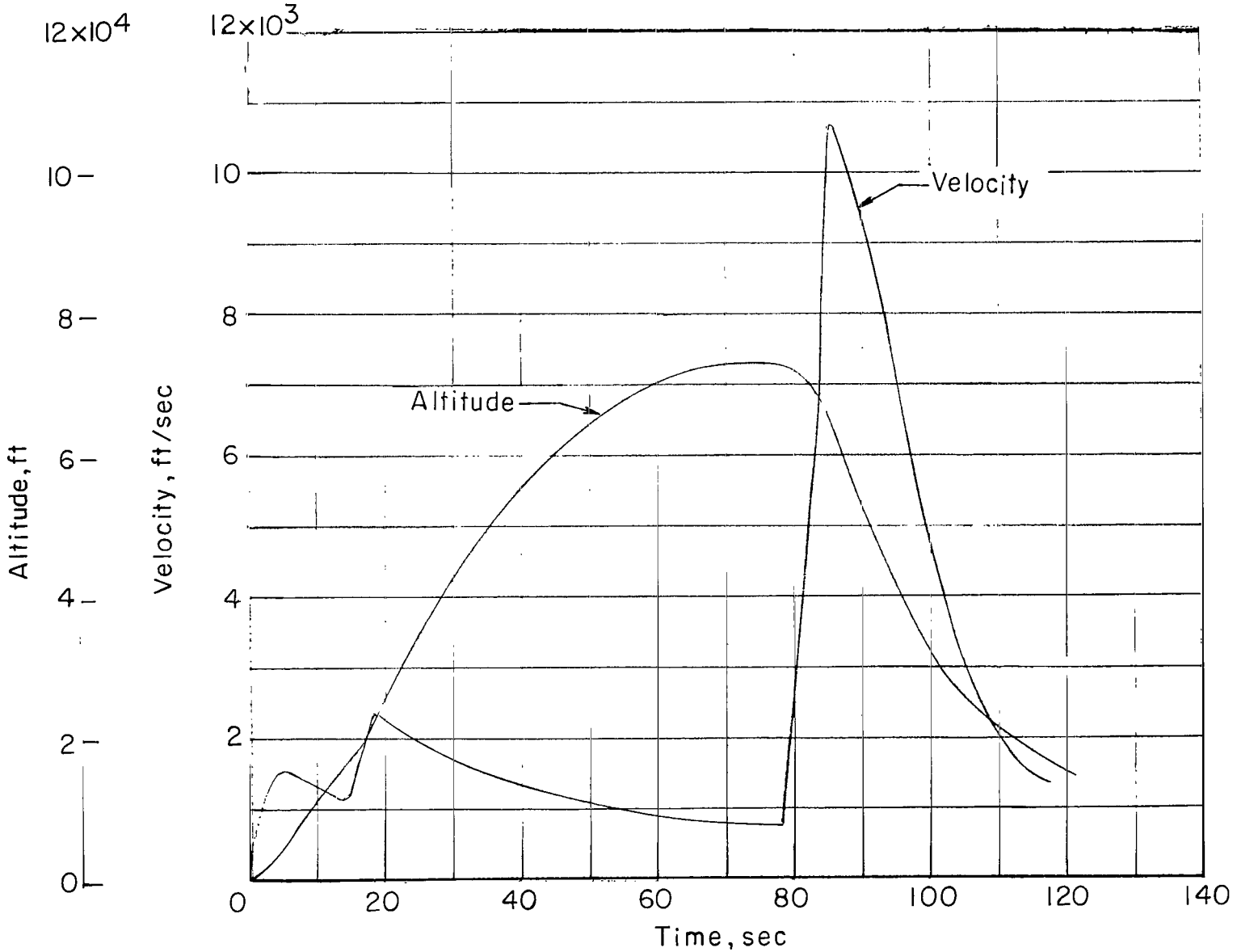

Figure 27.- Trajectory of the fourth-stage recoverable nose.

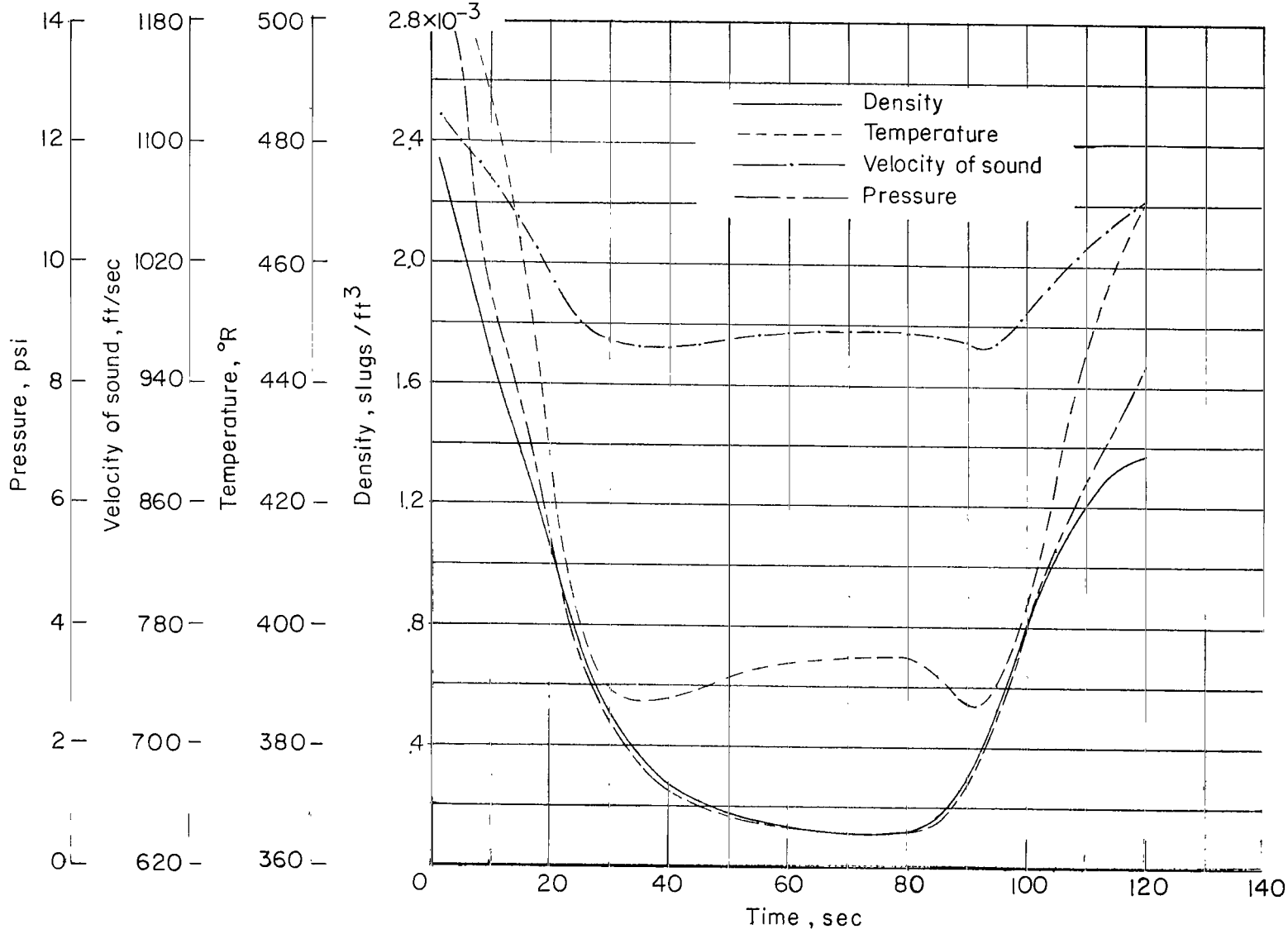

Figure 28.- Measured atmospheric conditions for payload recovery flight.

Figure 29.- Recoverable payload after flight. L-63-3991

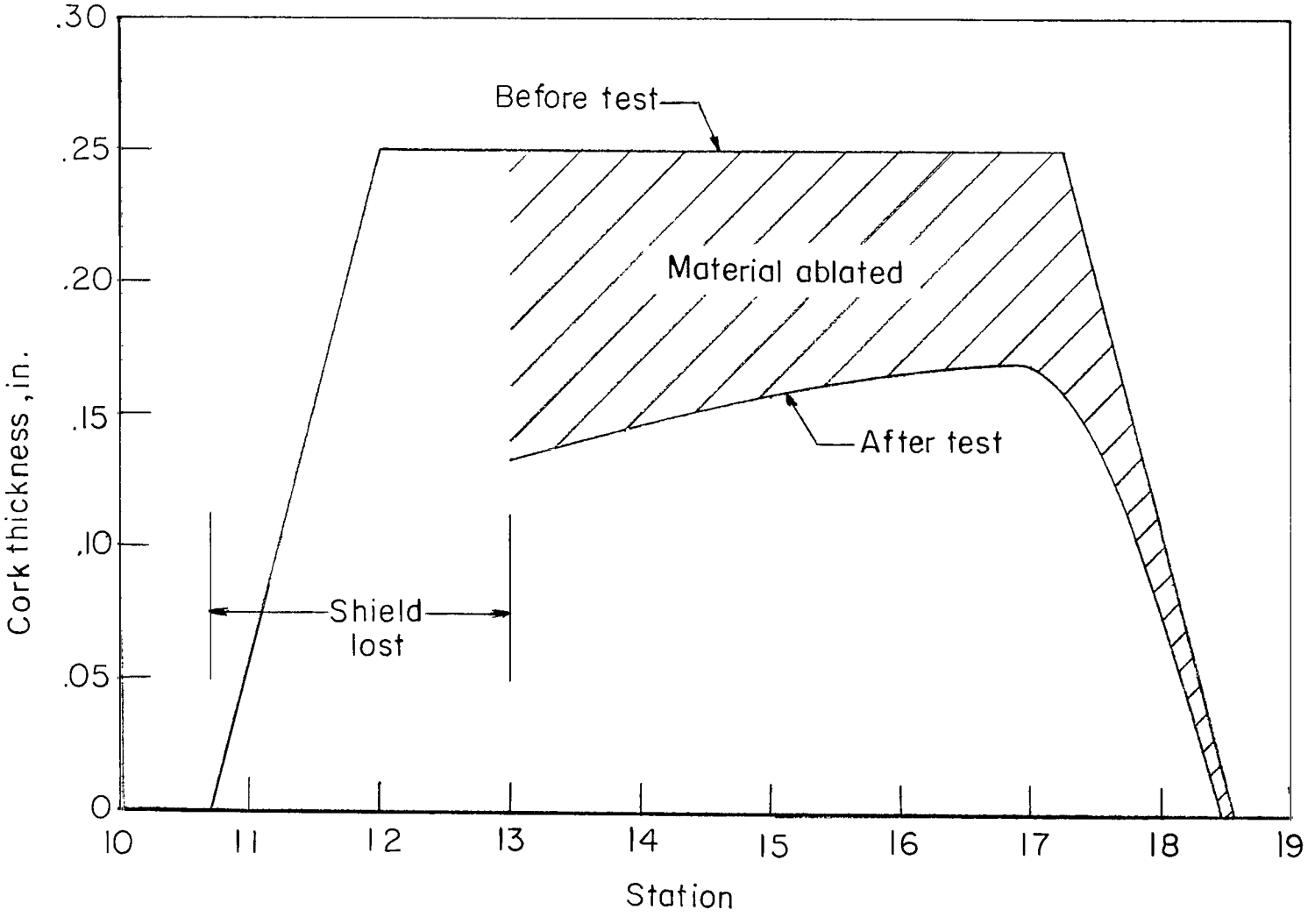

Figure 30.- Measured cork thickness, before and after test, for the recoverable payload.

"The aeronautical and space activities of the United States shall be conducted so as to contribute . . . to the expansion of human knowledge of phenomena in the atmosphere and space. The Administration shall provide for the widest practicable and appropriate dissemination of information concerning its activities and the results thereof."

—NATIONAL AERONAUTICS AND SPACE ACT OF 1958

NASA SCIENTIFIC AND TECHNICAL PUBLICATIONS

TECHNICAL REPORTS: Scientific and technical information considered important, complete, and a lasting contribution to existing knowledge.

TECHNICAL NOTES: Information less broad in scope but nevertheless of importance as a contribution to existing knowledge.

TECHNICAL MEMORANDUMS: Information receiving limited distribution because of preliminary data, security classification, or other reasons.

CONTRACTOR REPORTS: Technical information generated in connection with a NASA contract or grant and released under NASA auspices.

TECHNICAL TRANSLATIONS: Information published in a foreign language considered to merit NASA distribution in English.

TECHNICAL REPRINTS: Information derived from NASA activities and initially published in the form of journal articles.

SPECIAL PUBLICATIONS: Information derived from or of value to NASA activities but not necessarily reporting the results of individual NASA-programmed scientific efforts. Publications include conference proceedings, monographs, data compilations, handbooks, sourcebooks, and special bibliographies.

Details on the availability of these publications may be obtained from:

SCIENTIFIC AND TECHNICAL INFORMATION DIVISION

NATIONAL AERONAUTICS AND SPACE ADMINISTRATION

Washington, D.C. 20546